Ordinary differential equations for the adjoint Euler equations

Jacques Peter, Jean-Antoine Désidéri

Ordinary differential equations for the adjoint Euler equations

Jacques Peter*,[a], Jean-Antoine Désidéri[b]

[a] *DAAA, ONERA, Université Paris Saclay, F-92322 Châtillon, France*
[b] *Centre Inria Université Côte d'Azur, Inria, 2004 Route des Lucioles, BP 93, 06902 Sophia Antipolis, France*

Abstract

Ordinary Differential Equations are derived for the adjoint Euler equations firstly using the method of characteristics in 2D. For this system of partial-differential equations, the characteristic curves appear to be the streamtraces and the well-known $\mathscr{C}^+$and $\mathscr{C}^-$curves of the theory applied to the flow. The differential equations satisfied along the streamtraces in 2D are then extended and demonstrated in 3D by linear combinations of the original adjoint equations. These findings extend their well-known counterparts for the direct system, and should serve analytical and possibly numerical studies of the perfect-flow model with respect to adjoint fields or sensitivity questions. Beside the analytical theory, the results are demonstrated by the numerical integration of the compatibility relationships for discrete 2D flow-fields and dual-consistent adjoint fields over a very fine grid about an airfoil.

Key words: continuous adjoint method, compressible Euler equations, supersonic flow, charateristic curves

1. Introduction

In 1988, Jameson derived the continuous adjoint equations associated with the 2D and 3D Euler equations using general curvilinear coordinates [1]. With this landmark article, the fluid dynamics and aeronautical communities became better aware of the potential of the adjoint approach for design, that is, the possibility to calculate gradient information at a cost scaling with the number of functions to be differentiated, independently of the number of design parameters. The equations in [1] appeared to be a natural starting point for local optimizations involving a large number of design variables by using adjoint gradients. However, in that setting, the flow and the dual fields had to be calculated over a structured mesh.

Nine years later, Anderson and Venkatakrishnan [2, 3] and also Giles and Pierce [4] derived the corresponding equations in Cartesian coordinates thus allowing the application of the continuous approach (sometimes referred to as the differentiate-then-discretize approach) on all types of meshes and, in particular, on unstructured meshes. For the sake of simplicity, we present here the two-dimensional case only in which the adjoint equations read

$$-A^T \frac{\partial \psi}{\partial x} - B^T \frac{\partial \psi}{\partial y} = 0, \quad \text{in } \Omega \text{ the fluid domain} \tag{1}$$

where A and B are the Jacobian matrices of the flux vectors F_x and F_y of the Euler equations in the x and y directions respectively:

$$F_x = \begin{pmatrix} \rho u \\ \rho u^2 + p \\ \rho uv \\ \rho uH \end{pmatrix} \qquad F_y = \begin{pmatrix} \rho v \\ \rho uv \\ \rho v^2 + p \\ \rho vH \end{pmatrix},$$

with ρ the density, (u,v) the velocity components, p the static pressure and H the total enthalpy. In the most common case where the quantity of interest (QoI) is a line integral along the solid wall Γ_w, it can be shown easily that the adjoint

*Corresponding author. Tel.: +33 1 46 73 41 84.
Email addresses: jacques.peter@onera.fr (Jacques Peter), jean-antoine.desideri@inria.fr (Jean-Antoine Désidéri)

wall boundary condition is well-posed provided that the function of interest depends only on the static pressure [3]. In the classical case where the functional output of interest is the force on Γ_w projected in direction $\overline{d}$, $J = \int_{\Gamma_w} p(\overline{n}\cdot\overline{d})ds$, the wall boundary condition reads

$$\overline{n}\cdot\overline{d} + \psi_2 n_x + \psi_3 n_y = 0 \quad \text{on } \Gamma_w. \tag{2}$$

For the farfield of an external flow, as well as for the inlet and outlet of an internal flow, the boundary conditions are derived from the theory of local one-dimensional characteristic decomposition [2, 5]. Here, the continuous adjoint Euler equations and the associated boundary conditions are abbreviated as (AE). Along with the growing use of the adjoint method for shape optimization, goal oriented mesh adaptation and also meta-modelling, stability or control, great effort is being devoted to gain understanding in the mathematical properties of the (AE) solutions. The main results are summarized here before discussing the characteristic relations for the (AE) system.

After the derivation of the (AE) equations, the first demonstrated property was also due to Giles and Pierce [4]: in the common case where the function of interest is an integral along the wall, the authors proved that the first and last components of the adjoint vector ψ, associated with mass and energy conservation, satisfy $\psi_1 = H\psi_4$.

Besides, the integration by parts yielding (1) is not valid in the entire fluid domain in the presence of flow discontinuities. After a series of works dealing with the quasi-1D Euler equations – see [5, 6] and references therein – Baeza et al. presented the equations complementing (1) along a shock line [6] (denoted here Σ as in the original reference). The new equations are derived by introducing a complementary set of Lagrange multipliers, multiplying the Rankine-Hugoniot conditions, viewed as constraints on Σ. Finally, the continuity of the adjoint field ψ along Σ is established, although $\nabla\psi$ may be discontinuous across Σ, as well as ψ over $\Gamma_w \cap \Sigma$, and a so-called internal boundary condition is derived:

$$(\partial\psi/\partial t).(F_x t_x + F_y t_y) = 0 \qquad \text{on} \qquad \Sigma \tag{3}$$
$$\text{with } t \text{ the unit vector tangent to } \Sigma$$

Coquel et al., Lozano and Renac [7, 8, 9] have derived additional relationships by using (3), the jump operator applied to (1) across Σ and the Rankine-Hugoniot equations.

The fact that $\psi_1 = H\psi_4$ can be proven simply by forming the linear combination of the first three lines of system (1) with coefficients $(1, u/2, v/2)$. This yields $\overline{U}.\nabla\psi_1 - H\overline{U}.\nabla\psi_4 = 0$ (with $\overline{U} = (u,v)$ the velocity vector). Note that this was also derived in [4] by an approach based on physical source terms, constituting an important analysis technique for the adjoint field of usual QoIs. In particular, this method proved to be very fruitful to identify the zones where numerical divergence of the adjoint vector is observed and mathematical divergence of the solutions of (AE) is suspected. For the sake of clarity and brevity, we restrict the present discussion to 2D flows about lifting airfoils, and to two of these zones, namely the stagnation streamline and the wall, and to the lift and drag as functions of interest.

More precisely, Giles and Pierce [4] introduced four physical punctual source terms (or Green's functions in the classical mathematical vocabulary) denoted here δR^1, δR^2, δR^3, δR^4. These terms are added to the right hand-side of the linearised Euler equations and correspond respectively to *(i)* a mass source at fixed stagnation pressure p_0 and enthalpy H ; *(ii)* a normal force ; *(iii)* a change in H at fixed p and p_0; and *(iv)* a change in p_0 at fixed p and H. They are linearly independent. (We refer to the original reference for the detailed expression of these source terms.) The resulting changes in the QoI J, δJ^l, can be expressed as the integral over the domain of $\psi\delta R^l$ that is, the value at the source location since δR^l is a Green's function. These source terms also admit a physical interpretation and their influence on the flow can be understood in terms of mechanical principles, and sometimes even quantified finally providing insight in the adjoint field [4].

It has been observed that the lift adjoint exhibits numerical divergence at the stagnation streamline and at the wall at subcritical flow conditions. Also the drag and lift adjoint of a transonic airfoil exhibit numerical divergence at the same locations if the foot of at least one shock wave is located strictly upwind the trailing edge – see [10, 11] and references therein. Reference [9] includes a careful verification of this physical perturbations approach applied to the discrete adjoint with a preliminary assessment of the consistency between the linear (discrete adjoint) and the non-linear (flow perturbation) evaluations of the δJ^l. After this verification step, the non-linear perturbed flow approach has been used (considering the physical source terms point of view prior to the classical adjoint) and it appeared that: (a) δR^4 is the only source term causing a numerical divergence of δJ in the vicinity of the wall and stagnation streamline ; (b) in transonic condition, the numerical divergence of δCLp^4 and δCDp^4 in these zones is mainly due

to the displacement of the shockfoot (or shock-feet if two shocks are not based at the trailing edge) ; (c) this numerical divergence is transferred to the adjoint components via the inverse matrix of the source terms ; (d) this does not necessarily prevent the numerical satisfaction of the adjoint lift- (resp. drag-) boundary condition at the wall (2) as the calculation of $\psi_2 n_x + \psi_3 n_y$ in this approach involves the product of δCLp^4 (resp. δCDp^4) by $(un_x + vn_y)$.

The method of characteristics for 2D inviscid supersonic flow is a classical method for deriving ordinary differential equations and, potentially, explicit algebraic relations satisfied along two families of curves, denoted $\mathscr{C}^+$(left running with respect to (w.r.t.) a streamline) and $\mathscr{C}^-$(right running). Here, we recall the derivation of the continuous equations and study their counterparts for the (AE) equations.
For the flow, the method starting point is the Cauchy problem posed for the Euler equations: knowing the state variables along a fixed curve (L), is it possible to calculate their partial derivatives, in both space directions, for all points of (L) (this being a necessary condition for the flow calculation in the fluid domain) ? The flow variables in two neighboring points of (L), denoted here a and b, are linked by fluid dynamics equations and basic first order Taylor formulas. The more general presentations deal with rotational flows and, geometrically, both planar and axisymmetrical flows [12, 13, 14, 15]. The authors derive a system of equations for the derivatives of selected primitive variables. This system is linear in the unknown partial derivatives with non linear functions of the state variables as coefficients. When its determinant is equal to zero, it cannot be solved. That is the case if b is on the streamline of a or, in case of a supersonic flow, if the angle of $\overrightarrow{ab} = (dx, dy)$ w.r.t. the streamline passing through a is $\pm\sin^{-1}(1/M)$ (M being the local Mach number). The specific curves (L) where these conditions are satisfied for every points are, for all Mach numbers, the streamtraces, and, where the flow is supersonic, the so-called $\mathscr{C}^+$(left running curves w.r.t. the streamtraces with angle $\sin^{-1}(1/M)$) and the $\mathscr{C}^-$(right running curves the w.r.t. streamtraces with angle $-\sin^{-1}(1/M)$). Along these curves, the physical existence and boundedness of the vector of unknowns allows to conclude from the nullity of the determinant in the denominator of Cramer's formulas, to the nullity of the determinants appearing in the numerators, and this, for all the variables. The classical computational method for supersonic flow [12, 13, 16, 14, 17, 15] is supported by the corresponding differential forms valid along the $\mathscr{C}^+$and $\mathscr{C}^-$curves, and the property of constant total enthalpy and constant entropy along the streamtraces. If the flow is irrotational, homoenthalpic and homoentropic, simpler equations are derived for the velocity magnitude and the velocity angle [13, 18, 16] or the velocity potential [17] and the differential forms satisfied along the $\mathscr{C}^+$and $\mathscr{C}^-$curves may be integrated. This permits to establish the well-known equations

$$k^- = \phi + \nu(M) \text{ is constant along a } \mathscr{C}^- \qquad k^+ = \phi - \nu(M) \text{ is constant along a } \mathscr{C}^+ \tag{4}$$

in which ϕ is the streamline angle, $\nu(M)$ the Prandtl-Meyer function,

$$\phi = \tan^{-1}(v/u), \quad \nu(M) = \sqrt{\frac{\gamma+1}{\gamma-1}}\tan^{-1}\Big(\sqrt{\frac{\gamma-1}{\gamma+1}(M^2-1)}\Big) - \tan^{-1}\big(\sqrt{M^2-1}\big),$$

and γ the ratio of specific heats ($\gamma = \frac{7}{5}$ for diatomic perfect gas). Finally, let us recall that the integration of the corresponding ODEs along the trajectories results in the property of constant enthalpy and constant entropy.
Besides, Bonnet and Luneau indicate that the mechanical equations posed in a may be expressed in the Cartesian frame of reference rather than in the usual local frame derived from the local velocity [14]. Note that the 2D characteristic equations could also be calculated in the Cartesian frame and in an inexpert way, without taking advantage of the known properties of the streamtraces. Then the following the 8×8 linear system relating the derivatives of the conservative variables would be solved:

$$\begin{bmatrix} dx & 0 & 0 & 0 & dy & 0 & 0 & 0 \\ 0 & dx & 0 & 0 & 0 & dy & 0 & 0 \\ 0 & 0 & dx & 0 & 0 & 0 & dy & 0 \\ 0 & 0 & 0 & dx & 0 & 0 & 0 & dy \\ & & & & & & & \\ & & & & & & & \\ & & A & & & & B & \\ & & & & & & & \end{bmatrix} \begin{bmatrix} (\partial\rho/\partial x) \\ (\partial\rho u/\partial x) \\ (\partial\rho v/\partial x) \\ (\partial\rho E/\partial x) \\ (\partial\rho/\partial y) \\ (\partial\rho u/\partial y) \\ (\partial\rho v/\partial y) \\ (\partial\rho E/\partial y) \end{bmatrix} = \begin{bmatrix} \rho^b - \rho^a \\ \rho u^b - \rho u^a \\ \rho v^b - \rho v^a \\ \rho E^b - \rho E^a \\ 0. \\ 0. \\ 0. \\ 0. \end{bmatrix} \tag{5}$$

The starting point of our analytical development resides in the observation that (5) and the corresponding linear system for the (AE) equations, (6), have the same determinant. From this observation, the adjoint Euler characteristics equations are established in Sec. 2. The theoretical findings are linked with former researches and illustrated by numerical computational solutions over a very fine grid in Sec. 3. Conclusions are drawn in Sec. 4.

2. Adjoint characteristic equations for 2D supersonic flow

The method exposed in [17] (resp. [15]) for potential (resp. general) inviscid flow has served as a guideline to our derivation for the adjoint system. For all our calculations, we assume an ideal gas law for the static pressure $p=(\gamma-1)\rho e=(\gamma-1)(\rho E-0.5\rho||\overline{U}||^2)$ with a constant γ.

2.1. Problem statement

Given two fixed close points in the supersonic zone, a and b, is it possible to estimate $(\partial\psi/\partial x),(\partial\psi/\partial y)$ from the local value of the flow field and (ψ_a,ψ_b) ? This question is the starting point of the method of characteristics in which specific lines are identified along which this problem is ill-posed, and particular ordinary differential equations are satisfied. Let us denote $\overrightarrow{ab}=(dx,dy)$ and first assume that $dx\neq 0$. By definition of differential forms, and in view of the adjoint system (1), the following holds

$$\begin{bmatrix} dx & 0 & 0 & 0 & dy & 0 & 0 & 0 \\ 0 & dx & 0 & 0 & 0 & dy & 0 & 0 \\ 0 & 0 & dx & 0 & 0 & 0 & dy & 0 \\ 0 & 0 & 0 & dx & 0 & 0 & 0 & dy \\ & & & & & & & \\ & & & & & & & \\ & - & A^T & & & - & B^T & \\ & & & & & & & \end{bmatrix} \begin{bmatrix} (\partial\psi_1/\partial x) \\ (\partial\psi_2/\partial x) \\ (\partial\psi_3/\partial x) \\ (\partial\psi_4/\partial x) \\ (\partial\psi_1/\partial y) \\ (\partial\psi_2/\partial y) \\ (\partial\psi_3/\partial y) \\ (\partial\psi_4/\partial y) \end{bmatrix} = \begin{bmatrix} d\psi_1 \\ d\psi_2 \\ d\psi_3 \\ d\psi_4 \\ 0 \\ 0 \\ 0 \\ 0 \end{bmatrix} \tag{6}$$

in which by neglecting second-order terms in space: $(d\psi_1,d\psi_2,d\psi_3,d\psi_4)=(\psi_1^b-\psi_1^a,\psi_2^b-\psi_2^a,\psi_3^b-\psi_3^a,\psi_4^b-\psi_4^a)$. The determinant of the linear system is evidently

$$\begin{vmatrix} dxI & dyI \\ -A^T & -B^T \end{vmatrix} = \begin{vmatrix} dxI & 0 \\ -A^T & -B^T+dy/dxA^T \end{vmatrix} = dx^4|-B^T+dy/dxA^T| = |-dxB^T+dyA^T|$$

Of course, $|-dxB^T+dyA^T|$ is equal to $|-dxB+dyA|$ and the value of this determinant is known from the eigenvalues of the matrix:

$$D=|-dxB+dyA|=(-v\,dx+u\,dy)^2(-v\,dx+u\,dy+c\,ds)(-v\,dx+u\,dy-c\,ds),$$

in which

$$c=\sqrt{\frac{\gamma p}{\rho}},\quad ds=\sqrt{dx^2+dy^2}.$$

Similarly to the flow derivatives reconstruction [17, 15], the problem of adjoint derivatives reconstruction in a supersonic zone is ill-posed along the same three families of curves

$$-v\,dx+u\,dy = 0 \qquad \mathscr{S} \text{ streamtraces} \qquad \text{(all Mach numbers)} \tag{7}$$

$$-v\,dx+u\,dy+c\,ds = 0 \qquad \mathscr{C}^- \text{characteristics} \qquad \text{(supersonic flow only)} \tag{8}$$

$$-v\,dx+u\,dy-c\,ds = 0 \qquad \mathscr{C}^+ \text{characteristics} \qquad \text{(supersonic flow only)} \tag{9}$$

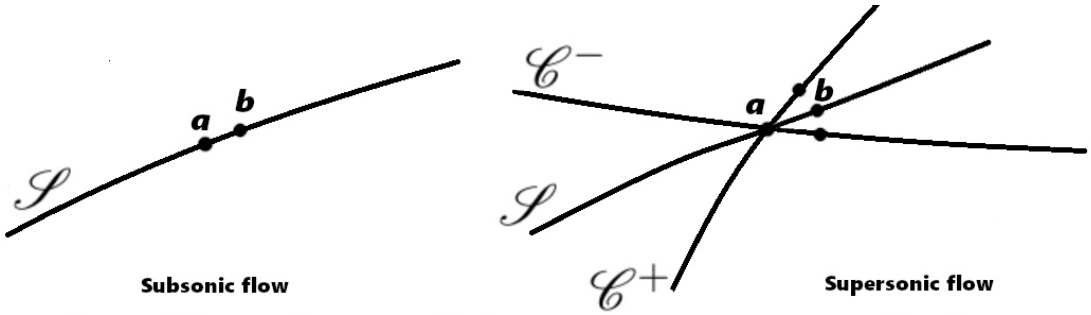

Figure 1: $\mathscr{S}$, $\mathscr{C}^+$ and $\mathscr{C}^-$ curves according to local Mach number. Neighboring a and b points along these curves

Classically, the method of characteristics uses the ill-posedness of (6) in the following way: along the curves defined by equations (7), (8) or (9), not only the denominator appearing in the Cramer formulas applied to the linear equations (6) is equal to zero, but the numerators giving the eight components of $(\partial\psi/\partial x)$ and $(\partial\psi/\partial y)$ must also be equal to zero for the fractions not to be singular. This (somehow paradoxical) technique allows the derivation of equations (4). It is derived here for the (AE) system by analysing the set of linear equations (6).

2.2. Null differential forms in the adjoint variations along trajectories and characteristics

The transposed of the Euler flux Jacobian matrices in x and y direction read

$$A^T = \begin{bmatrix} 0 & \gamma_1 E_c - u^2 & -uv & (\gamma_1 E_c - H)u \\ 1 & (3-\gamma)u & v & H - \gamma_1 u^2 \\ 0 & -\gamma_1 v & u & -\gamma_1 uv \\ 0 & \gamma_1 & 0 & \gamma u \end{bmatrix} \qquad B^T = \begin{bmatrix} 0 & -uv & \gamma_1 E_c - v^2 & (\gamma_1 E_c - H)v \\ 0 & v & -\gamma_1 u & -\gamma_1 uv \\ 1 & u & (3-\gamma)v & H - \gamma_1 v^2 \\ 0 & 0 & \gamma_1 & \gamma v \end{bmatrix}$$

in the usual notations in aerodynamics and $\gamma_1 = \gamma - 1$. Let

$$t = \frac{dy}{dx}, \quad \kappa = ut - v,$$

and also introduce the following notations for the column vectors of the transposed Jacobian matrices: $A^T = [A_1|A_2|A_3|A_4]$, $B^T = [B_1|B_2|B_3|B_4]$. Before presenting the results, the principle of the calculation is recalled in one of the cases that leads to the simplest calculations: the definition of $(\partial\psi_4/\partial x)$ along the curves where (7), (8) or (9) is satisfied (that is, the streamtraces, the $\mathscr{C}^-$ or $\mathscr{C}^+$ characteristic) requires that, along these curves

$$\begin{vmatrix} dx & 0 & 0 & d\psi_1 & dy & 0 & 0 & 0 \\ 0 & dx & 0 & d\psi_2 & 0 & dy & 0 & 0 \\ 0 & 0 & dx & d\psi_3 & 0 & 0 & dy & 0 \\ 0 & 0 & 0 & d\psi_4 & 0 & 0 & 0 & dy \\ | & | & | & | & | & | & | & | \\ -A_1 & -A_2 & -A_3 & 0 & -B_1 & -B_2 & -B_3 & -B_4 \\ | & | & | & | & | & | & | & | \end{vmatrix} = 0$$

The determinant is expanded along the fourth column and the following notations are used

$$-C^1_{4x} d\psi_1 + C^2_{4x} d\psi_2 - C^3_{4x} d\psi_3 + C^4_{4x} d\psi_4 = 0 \tag{10}$$

in which, for example

$$C^1_{4x} = \begin{vmatrix} 0 & dx & 0 & 0 & dy & 0 & 0 \\ 0 & 0 & dx & 0 & 0 & dy & 0 \\ 0 & 0 & 0 & 0 & 0 & 0 & dy \\ | & | & | & | & | & | & | \\ -A_1 & -A_2 & -A_3 & -B_1 & -B_2 & -B_3 & -B_4 \\ | & | & | & | & | & | & | \end{vmatrix} = \begin{vmatrix} 0 & dx & 0 & 0 & 0 & 0 & 0 \\ 0 & 0 & dx & 0 & 0 & 0 & 0 \\ 0 & 0 & 0 & 0 & 0 & 0 & dy \\ | & | & | & | & | & | & | \\ -A_1 & -A_2 & -A_3 & -B_1 & -B_2+tA_2 & -B_3+tA_3 & -B_4 \\ | & | & | & | & | & | & | \end{vmatrix}$$

Finally

$$C^1_{4x} = dx^2dy \mid \ -A_1 \ \ -B_1 \ \ (-B_2+tA_2) \ \ (-B_3+tA_3) \ \mid$$

The determinant of this 4×4 matrix is easily calculated thanks to the simplicity of the first two columns A_1 and B_1. The final result is

$$C^1_{4x} = dx^2dy \ \gamma_1 \ \kappa \ (u+vt)$$

We emphasise that at this stage no assumption is made on the value of $t = dy/dx$ w.r.t. the velocity vector (u,v). In particular t is not assumed to be the tangent of the angle of the velocity w.r.t. the x axis and κ is not assumed to be zero. This is mandatory to derive relations that can be used for all three types of specific curves and also to account for the multiplicity of the eigenvalue $(-v\,dx+u\,dy)$ along streamtraces. The other terms of the differential form of interest read

$$\begin{aligned} C^2_{4x} &= -dx^2dy \mid \ -A_2 \ \ (-B_1+tA_1) \ \ -B_2 \ \ (-B_3+tA_3) \ \mid = -dx^2dy \ \gamma_1 \ \kappa \ (u^2+v^2) \\ C^3_{4x} &= dx^2dy \mid \ -A_3 \ \ (-B_1+tA_1) \ \ (-B_2+tA_2) \ \ -B_3 \ \mid = dx^2dy \ \gamma_1 \ \kappa\, t \ (u^2+v^2) \\ C^4_{4x} &= dx^3 \mid \ (-B_1+tA_1) \ \ (-B_2+tA_2) \ \ (-B_3+tA_3) \ \ -B_4 \ \mid \\ &= -dx^3\kappa\big((\gamma_1+\gamma t^2)u^2v - 2uv^2t + \gamma_1 H\kappa + (\gamma+\gamma_1 t^2)v^3 - \gamma_1 v\,(1+t^2)\,E_c\big) \end{aligned}$$

The explicit expression of (10), the necessary condition for the boundedness of $(\partial\psi_4/\partial x)$, hence reads

$$\begin{aligned} &- \ dx^2dy \ \gamma_1 \ \kappa \ (u+vt) \ d\psi_1 - dx^2dy \ \gamma_1 \ \kappa \ (u^2+v^2)d\psi_2 - dx^2dy \ \gamma_1 \ \kappa\, t \ (u^2+v^2)d\psi_3 \\ &- \ dx^3\kappa\big((\gamma_1+\gamma t^2)u^2v - 2uv^2t + \gamma_1 H\kappa + (\gamma+\gamma_1 t^2)v^3 - \gamma_1 v\,E_c\,(1+t^2)\big)\,d\psi_4 = 0 \end{aligned} \tag{11}$$

Assuming that $dx \neq 0$, this equation may be further simplified for the $\mathscr{C}^-$ and $\mathscr{C}^+$ for which $\kappa \neq 0$:

$$\begin{aligned} &\gamma_1\, t(u+vt)\, d\psi_1 + \gamma_1\, t(u^2+v^2)\, d\psi_2 + \ \gamma_1\, t^2\ (u^2+v^2)\, d\psi_3 \\ + \ &\big((\gamma_1+\gamma t^2)u^2v - 2uv^2t + \gamma_1 H\kappa + (\gamma+\gamma_1 t^2)v^3 - \gamma_1 v\,E_c\,(1+t^2)\big)\,d\psi_4 = 0. \end{aligned} \tag{12}$$

As $(-v\,dx+u\,dy) = \kappa\,dx$ has a multiplicity of two in the determinant of (6), equation (12) is also needed for the existence of $(\partial\psi_4/\partial x)$ and hence true for neighboring points a and b along the same $\mathscr{S}$curves. (This point is detailed in §2.3.)

For the sake of clarity, the results of the corresponding calculations for the existence of the seven other partial derivatives along the $\mathscr{S}$, $\mathscr{C}^-$ and $\mathscr{C}^+$curves, and the properties of the $C^i_{jx}\,C^i_{jy}$ coefficients are presented in Appendix A and B. Only the counterparts of equation (12), for the existence of $(\partial\psi_1/\partial x)$, $(\partial\psi_2/\partial x)$, $(\partial\psi_3/\partial x)$, $(\partial\psi_1/\partial y)$, $(\partial\psi_2/\partial y)$, $(\partial\psi_3/\partial y)$ and $(\partial\psi_4/\partial y)$ are presented hereafter in this order:

$$\begin{aligned} &((2tu+(t^2-1)v)(\gamma_1 H+\gamma_1 E_c+\gamma v\kappa) - (u+vt)(\gamma_1 tH+\gamma_1 u\kappa+\gamma v\kappa t)d\psi_1 \\ + \ &\gamma_1\ t\ (u^2+v^2)\ H(d\psi_2+td\psi_3) + \gamma_1\ t\ (u+vt)\ H^2 d\psi_4 = 0 \end{aligned} \tag{13}$$

$$\begin{aligned} &t\ (\gamma_1 H+\gamma_1 E_c+\gamma v\kappa)\ (d\psi_1+Hd\psi_4) \\ - \ &(\gamma_1 u^2v - uv^2t + \gamma v^3 - \gamma_1(ut+v)(E_c+H))\ (d\psi_2+td\psi_3) = 0 \end{aligned} \tag{14}$$

$$\begin{aligned} &t\ (t\gamma_1 H+t\gamma_1 E_c-\gamma u\kappa)(d\psi_1+Hd\psi_4) + t\ ((\gamma+1)u^2v - t\gamma_1 uv^2 + (v+ut)(\gamma_1 E_c+\gamma_1 H-\gamma u^2))d\psi_2 \\ + \ &((tv^2-u\kappa)(-\gamma_1 u+(\gamma+1)tv) - (ut-(1+2t^2)v)(\gamma_1 E_c+\gamma_1 H-\gamma v^2))d\psi_3 = 0 \end{aligned} \tag{15}$$

$$\begin{aligned}
&\left((\gamma_1+\gamma t^2)u^3-2u^2vt-\gamma_1 t\kappa H+(\gamma+\gamma_1 t^2)uv^2-\gamma_1 u\,(1+t^2)\,E_c\right)d\psi_1\\
+\quad&\gamma_1\,(u^2+v^2)\,H(d\psi_2+td\psi_3)+\,\gamma_1\,(u+vt)\,H^2 d\psi_4=0
\end{aligned}\tag{16}$$

$$\begin{aligned}
&(\gamma_1 H+\gamma_1 E_c+\gamma v\kappa)\,(d\psi_1+Hd\psi_4)\\
+\quad&((v\kappa+u^2)(vt-(\gamma_1+\gamma t^2)u)-(vt-(2+t^2)u)(\gamma_1 E_c+\gamma_1 H+\gamma v\kappa))d\psi_2\\
-\quad&(\gamma_1 u^2 v-uv^2 t+\gamma v^3-\gamma_1(ut+v)(E_c+H))d\psi_3=0
\end{aligned}\tag{17}$$

$$\begin{aligned}
&(t\gamma_1 H+t\gamma_1 E_c-\gamma u\kappa)(d\psi_1+Hd\psi_4)\\
+\quad&((\gamma+1)u^2 v-t\gamma_1 uv^2+(v+ut)(\gamma_1 E_c+\gamma_1 H-\gamma u^2))(d\psi_2+td\psi_3)=0
\end{aligned}\tag{18}$$

$$\begin{aligned}
&\gamma_1\,(u+vt)\,d\psi_1+\gamma_1\,(u^2+v^2)(d\psi_2+td\psi_3)\\
+\quad&\left((\gamma_1+\gamma t^2)u^3-2u^2vt-\gamma_1 t\kappa H+(\gamma+\gamma_1 t^2)uv^2-\gamma_1 u\,E_c\,(1+t^2)\right)d\psi_4=0
\end{aligned}\tag{19}$$

2.3. Ordinary differential equations for the adjoint along the streamtraces $\mathscr{S}$

The trajectories are one of the families of specific curves for the gradient calculation problem (6). Along these curves $u\,dy-v\,dx=0$ is a zero of the denominator of Cramer's formulas with multiplicity two. Let us first assume that point a is fixed and point b is very close to $\mathscr{S}_a$, the streamtrace passing through a but not on this curve. The first-order expression of $(\partial\psi_1/\partial x)$ is

$$\frac{\partial\psi_1}{\partial x}=\frac{C^1_{1x}d\psi_1-C^2_{1x}d\psi_2+C^3_{1x}d\psi_3-C^4_{1x}d\psi_4}{(-v\,dx+u\,dy)^2(-v\,dx+u\,dy+c\,ds)(-v\,dx+u\,dy-c\,ds)}$$

Actually $\kappa dx=u\,dy-v\,dx$ is a factor of all four coefficients C^1_{1x}, C^2_{1x}, C^3_{1x} and C^4_{1x}. We denote by $\bar{C}^l_{mx}$ the coefficients obtained by removing the $(\kappa\,dx)$ factor from the corresponding C^l_{mx}. Obviously

$$\frac{\partial\psi_1}{\partial x}=\frac{\bar{C}^1_{1x}d\psi_1-\bar{C}^2_{1x}d\psi_2+\bar{C}^3_{1x}d\psi_3-\bar{C}^4_{1x}d\psi_4}{(-v\,dx+u\,dy)(-v\,dx+u\,dy+c\,ds)(-v\,dx+u\,dy-c\,ds)}$$

If point b is moved closer and closer to $\mathscr{S}_a$ $(-v\,dx+u\,dy)\to 0$, so that the boundedness of $(\partial\psi_1/\partial x)$ requires that

$$\bar{C}^1_{1x}d\psi_1-\bar{C}^2_{1x}d\psi_2+\bar{C}^3_{1x}d\psi_3-\bar{C}^4_{1x}d\psi_4=0\qquad\text{on}\quad\mathscr{S}_a$$

This expression and its counterparts for the other derivatives $(\partial\psi_2/\partial x)$ ... $(\partial\psi_4/\partial y)$ have to be satisfied for all trajectories. How many of these eight differential forms are independent ? If $\kappa\,dx=0$, then

$$\bar{C}^1_{1x}=-t\,\bar{C}^1_{1y}\quad\bar{C}^2_{2x}=-t\,\bar{C}^2_{2y}\quad\bar{C}^3_{3x}=-t\,\bar{C}^3_{3y}\quad\bar{C}^4_{4x}=-t\,\bar{C}^4_{4y}\tag{20}$$

as in this case

$$\bar{C}^1_{1x}=\bar{C}^4_{4x}=-0.5\,t\gamma_1 dx^2(1+t^2)^2u^3\qquad\bar{C}^1_{1y}=\bar{C}^4_{4y}=0.5\,\gamma_1 dx^2(1+t^2)^2u^3$$

$$\bar{C}^2_{2x}=2\,dx^2\gamma_1 tuH\quad\bar{C}^2_{2y}=-2\,dx^2\gamma_1 uH\qquad\bar{C}^3_{3x}=2\,dx^2\gamma_1 t^3uH\quad\bar{C}^3_{3y}=-2\,dx^2\gamma_1 t^2uH.$$

Relations (39) to (42) are valid for the $\bar{C}$ coefficients (as they stand whatever the values of w and dx, they may be simplified by wdx). In the specific case where $\kappa=0$ they are completed by (20). Equations {(16),(17),(18),(19)} (necessary for the boundedness of the $\partial\psi^l/\partial y$) and {(13),(14),(15),(12)} (same for $\partial\psi^l/\partial x$) are then proportional by a $(-t)$ factor. Considering the range of the set of the eight differential forms, it appears that one of these two sets of four equations need be accounted for.

The relations stemming from the existence of the ∂x partial derivative are retained. Equation (13), required for the definition of $(\partial\psi_1/\partial x)$, is further simplified using the specific properties of a trajectory ($\kappa=0$ $v=ut$):

$$0.5t\gamma_1(1+t^2)^2u^3d\psi_1+\,\gamma_1\,t\,(1+t^2)u^2\,H(d\psi_2+td\psi_3)+\,\gamma_1\,t\,(1+t^2)u\,H^2d\psi_4=0$$

$$0.5(1+t^2)u^2 d\psi_1 + u\,H(d\psi_2 + t d\psi_3) + H^2 d\psi_4 = 0$$

For the streamstraces, the equation finally derived from the existence of $(\partial\psi_1/\partial x)$ is

$$E_c\, d\psi_1 + H(u\, d\psi_2 + v\, d\psi_3) + H^2 d\psi_4 = 0 \tag{21}$$

Note that we have assumed that $u \neq 0$ and $dx \neq 0$ to perform the calculations but finally obtained an expression that is also well-defined in this specific case. Equation (14), is further simplified for the motion along a trajectory:

$$t\,(\gamma_1 H + \gamma_1 E_c)\,(d\psi_1 + H d\psi_4) + 2\gamma_1\, u\, t\, H\,(d\psi_2 + t d\psi_3) = 0$$

$$(H + E_c)\,(d\psi_1 + H d\psi_4) + 2H\,(u\, d\psi_2 + v\, d\psi_3) = 0$$

Using the first relation and simplifying by H, we get

$$H(d\psi_1 + H d\psi_4) + 2H\,(u\, d\psi_2 + v\, d\psi_3) + E_c H d\psi_4 - H(u d\psi_2 + v d\psi_3) - H^2 d\psi_4 = 0$$

$$\text{and finally} \qquad d\psi_1 + u\, d\psi_2 + v\, d\psi_3 + E_c d\psi_4 = 0 \tag{22}$$

Simplifying equation (15) for trajectories yields

$$(H + E_c)(d\psi_1 + H d\psi_4) + 2H(u d\psi_2 + v d\psi_3) = 0,$$

that had already been derived. Using $\kappa = 0$ and $v = ut$, the fourth relation (first simplified by a κdx factor) gives

$$\gamma_1\, tu(1+t^2)\, d\psi_1 + \gamma_1\, tu^2(1+t^2)\, d\psi_2 + \gamma_1 t^2\, u^2(1+t^2)\, d\psi_3 + 0.5t\gamma_1(1+t^2)^2 u^3 d\psi_4 = 0$$

$$\text{or} \qquad d\psi_1 + u\, d\psi_2 + tu\, d\psi_3 + 0.5(1+t^2)u^2 d\psi_4 = 0$$

$$\text{and finally} \qquad d\psi_1 + u\, d\psi_2 + v\, d\psi_3 + E_c\, d\psi_4 = 0$$

This equation is similar to (22). These differential forms along the trajectories $\mathscr{S}$ may be turned in differential equations. The natural variable w.r.t. which differentiate, is the curvilinear abscissa along the streamtraces, s, increasing in the direction opposite to the motion (as this is the direction of the adjoint transport of information from the support of the function of interest). The final equations along the $\mathscr{S}$ curves are then

$$E_c \frac{d\psi_1}{ds} + H(u \frac{d\psi_2}{ds} + v \frac{d\psi_3}{ds}) + H^2 \frac{d\psi_4}{ds} = 0 \tag{23}$$

$$\frac{d\psi_1}{ds} + u \frac{d\psi_2}{ds} + v \frac{d\psi_3}{ds} + E_c \frac{d\psi_4}{ds} = 0 \tag{24}$$

Although the calculations of this section are not very complex, they have been checked with the computer algebra software Maple. The independent variables of the formal calculations are (u, v) also M the Mach number (that allows the calculation of the speed of sound c and then the total enthalpy H) and γ. The set of four differential forms {(16), (17), (18), (19)} was associated with {(21),(22)} in a 6×4 matrix that was again found to have rank two.

2.4. Ordinary differential equation for the adjoint along the $\mathscr{C}^+$ and $\mathscr{C}^-$ characteristics

Let us first note that the determinant in the denominator of the Cramer formulas for (6) may be calculated as

$$D = dx\, C^1_{1x} + dy\, C^1_{1y}$$

developing D along the first line. Doing the same along the second, third and fourth lines yields

$$D = dx\, C^2_{2x} + dy\, C^2_{2y} = dx\, C^3_{3x} + dy\, C^3_{3y} = dx\, C^4_{4x} + dy\, C^4_{4y}$$

As $D = 0$ along the $\mathscr{C}^+$ and $\mathscr{C}^-$ characteristics, equations (39) to (42) are completed by

$$C^1_{1x} = -t\, C^1_{1y} \qquad C^2_{2x} = -t\, C^2_{2y} \qquad C^3_{3x} = -t\, C^3_{3y} \qquad C^4_{4x} = -t\, C^4_{4y}$$

so that the differential forms stemming from the boundedness of $(\partial\psi^l/\partial x)$ and their counterparts for $(\partial\psi^l/\partial x)$ are proportional. (Incidentally, note that this argument may have been used also in the previous subsection.)
Numerical tests indicate that the four differential forms associated with the existence of (choosing the second set) $(\partial\psi_1/\partial y)$, $(\partial\psi_2/\partial y)$, $(\partial\psi_3/\partial y)$, $(\partial\psi_4/\partial y)$ are proportional but the corresponding calculations are much more complex than in the previous subsection as the expression of t is now:

$$t^{\pm} = \tan(\phi+\beta) \quad \text{with} \quad \tan\phi = \frac{v}{u} \quad \sin\beta = \pm\frac{1}{M} \tag{25}$$

with, of course $\sin\beta = 1/M$ for the $\mathscr{C}^+$and $\sin\beta = -1/M$ for the $\mathscr{C}^-$curves.
With this expression of t and κ not being equal to zero, searching the rank of {(16), (17), (18), (19)} is much more difficult. However, the task was successfully accomplished with the assistance of Maple, using once again (u,v,M,γ) as independent formal variables. Rank one was indicated by Maple and the correspondence with the counterpart characteristics for the flow seemed very sound. Knowing this result from formal calculation, its demonstration by hand was searched for.
First, the value of t is calculated along the $\mathscr{C}^+$and $\mathscr{C}^-$curves. For β in $[-\pi/2,\pi/2]$ (25) yields

$$t^{\pm} = \frac{\dfrac{v}{u} \pm \dfrac{1}{\sqrt{M^2-1}}}{1 \mp \dfrac{v}{u}\dfrac{1}{\sqrt{M^2-1}}} = \frac{uvM^2 \pm (u^2+v^2)\sqrt{M^2-1}}{u^2(M^2-1)-v^2} = \frac{uv \pm c^2\sqrt{M^2-1}}{u^2-c^2} = \frac{uv \pm c\sqrt{u^2+v^2-c^2}}{u^2-c^2} \tag{26}$$

We then note that if the differential forms (16) and (19) were proportional, from the expressions of $C^2_{1y}, C^3_{1y}, C^2_{4y}$ and C^3_{4y}, the ratio between their terms would be $(-H)$. It is then easily checked that the two non-trivial conditions for proportionality, $C^1_{1y} = -HC^4_{1y}$ and $C^1_{4y} = -HC^4_{4y}$, are equivalent to a single equality

$$\gamma_1\ (u+vt)H = \left((\gamma_1+\gamma t^2)u^3 - 2u^2vt - \gamma_1 t\kappa H + (\gamma+\gamma_1 t^2)uv^2 - \gamma_1 u\ (1+t^2)\ E_c\right) \tag{27}$$

Wherever $u \neq 0$, this condition is equivalent to

$$\gamma_1\ (1+t^2)\ H = \gamma_1\ (1+t^2)\ E_c + (tu-v)^2 \tag{28}$$

that is, precisely, the degree two equation which roots are the values of t along the $\mathscr{C}^+$and $\mathscr{C}^-$curves (26). Along these curves, using (27) that is now an established property along the $\mathscr{C}^+$and $\mathscr{C}^-$, these two differential forms may be simplified as

$$(u+vt^{\pm})\ d\psi_1 + (u^2+v^2)(d\psi_2 + t^{\pm}d\psi_3) + H(u+vt^{\pm})\ d\psi_4 = 0, \tag{29}$$

or, under the form of an ordinary differential equation,

$$(u+vt^{\pm})\ \frac{d\psi_1}{ds} + (u^2+v^2)\left(\frac{d\psi_2}{ds} + t^{\pm}\frac{d\psi_3}{ds}\right) + H(u+vt^{\pm})\ \frac{d\psi_4}{ds} = 0. \tag{30}$$

Comparing equations (18) – expressing the boundedness of $(\partial\psi_3/\partial y)$ – and (29) – its counterpart for $(\partial\psi_1/\partial y)$ and $(\partial\psi_4/\partial y)$) – it is easily derived that these equations are proportional on the $\mathscr{C}^+$and $\mathscr{C}^-$curves if and only if for $t = t^{\pm}$

$$(t\gamma_1 H + t\gamma_1 E_c - \gamma u\kappa)(u^2+v^2) = ((\gamma+1)u^2v - t\gamma_1 uv^2 + (v+ut)(\gamma_1 E_c + \gamma_1 H - \gamma u^2))(u+vt)$$

Wherever $uv \neq 0$, this equation is equivalent to

$$\gamma(u^2+v^2) = ((\gamma+1)u - t\gamma_1 v)(u+vt) + (\gamma_1 E_c + \gamma_1 H - \gamma u^2)(1+t^2)$$

that is found to be equivalent to equation (28), the degree two equation t which roots are the slope coefficients of the $\mathscr{C}^+$and $\mathscr{C}^-$. Equation (18) hence also reduces to (29) along the $\mathscr{C}^+$and $\mathscr{C}^-$curves.
Finally, we consider the last differential form (17), expressing the boundedness of $(\partial\psi_2/\partial y)$. Whether it is proportional to (29) is not straightforward in particular due to the complex expression of C^2_{2y} and the ratio C^3_{2y}/C^2_{2y} that is not

obviously equal to t. Nevertheless, we have proven that, along the characteristic curves the differential form expressing the boundedness of $(\partial\psi_2/\partial x)$ and $(\partial\psi_2/\partial y)$ (equations (14) and (17)) are proportional by a minus t factor. So we may use this property to derive a simpler expression of C_{2y}^2 or prove the proportionality of (14) with (29) along the $\mathscr{C}^+$and $\mathscr{C}^-$curves. Whatever the approach the condition for proportionality reads

$$t\ (\gamma_1 H+\gamma_1 E_c+\gamma v\kappa)(u^2+v^2)=(\gamma_1(ut+v)(E_c+H)+uv^2t-\gamma_1 u^2v-\gamma v^3)(u+vt),$$

that is found to be equivalent to (28) wherever $uv\neq 0$.
In a final formal calculation verification, it was checked that, on the $\mathscr{C}^+$and $\mathscr{C}^-$curves, (16), is proportional to (29) (and we already know that equations (17), (18), (19) are proportional to (16) along these curves).

2.5. Main results and extension to 3D

We have found two differential equations, (23) and (24), valid along the streamtraces $\mathscr{S}$for the adjoint system:

$$E_c\ \frac{d\psi_1}{ds}+H(u\ \frac{d\psi_2}{ds}+v\ \frac{d\psi_3}{ds})+\ H^2\frac{d\psi_4}{ds}=0 \qquad \frac{d\psi_1}{ds}+u\ \frac{d\psi_2}{ds}+v\ \frac{d\psi_3}{ds}+E_c\frac{d\psi_4}{ds}=0.$$

They are the counterpart of the constant total enthalpy and constant entropy properties for the flow. They may be combined (for example to derive again $\overline{U}.\nabla\psi_1-H\overline{U}.\nabla\psi_4=0$) or their coefficients may be expressed differently using the well-known equations satisfied by steady inviscid flows along a streamtrace. Let us finally note that their straightforward 3D extensions (with natural notations),

$$E_c\ \frac{d\psi_1}{ds}+H(u\ \frac{d\psi_2}{ds}+v\ \frac{d\psi_3}{ds}+w\ \frac{d\psi_4}{ds})+H^2\ \frac{d\psi_5}{ds}=0$$
$$\frac{d\psi_1}{ds}+u\ \frac{d\psi_2}{ds}+v\ \frac{d\psi_3}{ds}+w\ \frac{d\psi_4}{ds}+E_c\ \frac{d\psi_5}{ds}=0,$$

are valid. This is the subject of Appendix C. The demonstration used in 3D also provides another method for deriving the 2D equations.
We have found one differential equation for the $\mathscr{C}^+$and one differential equation for the $\mathscr{C}^-$, equation (30) with relevant value of $t^{\pm}$ for each curve (26)

$$(u+vt^{\pm})\ \frac{d\psi_1}{ds}+(u^2+v^2)(\frac{d\psi_2}{ds}+t^{\pm}\frac{d\psi_3}{ds})+H(u+vt^{\pm})\ \frac{d\psi_4}{ds}=0.$$
$$t^+=\frac{uv+c\sqrt{u^2+v^2-c^2}}{u^2-c^2}\quad\text{for a }\mathscr{C}^+ \qquad t^-=\frac{uv-c\sqrt{u^2+v^2-c^2}}{u^2-c^2}\quad\text{for a }\mathscr{C}^-$$

They are the counterpart of the differential forms satisfied by primitive flow variables along the $\mathscr{C}^+$and $\mathscr{C}^-$. In the simpler cases, where the classical angular relations (4) are valid, these relations may be used to express differently the coefficients. We do not expect these relations involving a 2D slope, t, to admit an extension in 3D.

3. Assessment of the adjoint ODEs

3.1. Consistency with known flow perturbation mechanisms

The adjoint vector is known to express the influence of a flow perturbation on the associated QoI. Although discrete and continuous adjoint methods are nowdays common tools for shape optimization, flow control and receptivity-sensitivity-stability analysis, adjoint vectors are not easily interpreted. The reason is that a single adjoint component, at a given location, is the rate of the change in the QoI to the amplitude of a local perturbation in the corresponding flow equation only (eg for the first component, mass injection without perturbation of the momentum and energy equations). These individual equation perturbations, of course, do not correspond to any realistic possibility. A second complementary point of view, already mentioned in the introduction, consists in calculating the dot product of the adjoint components with the vector of a realistic perturbation and discuss the map of the actuation influence [4, 9]. Plots of individual adjoint components for Euler flows appear in a 2002 publication by Venditti and Darmofal [19]

(fig. 19 and 26). The discussion of a x-momentum *CL*-adjoint plot in [19] mentions *a singularity in the adjoint along the stagnation streamline and a weak discontinuity upstream of the primal shock on the upper surface.* (With a finer mesh, the latter would have been identified as a $\mathscr{C}^-$impinging the upperside shock-foot). Although not discussed by the authors of [19], a corresponding plot for a supersonic flow about two airfoils, strongly suggest backward information propagation along the $\mathscr{S}$, $\mathscr{C}^-$and $\mathscr{C}^+$curves from the support of the QoI. Concerning transonic airfoil flows, reference [20] describes the mechanism by which locally perturbing one component of the flow along the $\mathscr{C}^-$(resp. $\mathscr{C}^+$) impinging the upperside (resp. lowerside) shock-foot results in a strong change in the lift and drag: the flow perturbation propagates along the $\mathscr{C}^-$(resp. $\mathscr{C}^+$) and results in a displacement of the shock.
The evaluation of the influence of physical source terms on the lift or drag of a profile goes back to Giles and Pierce [4] who introduced the four physical local source terms recalled in section I. Consistently with equations (23), (24) and (30) the results obtained with this approach also support adjoint information propagation along the $\mathscr{S}$, $\mathscr{C}^-$and $\mathscr{C}^+$, from the support of the QoI (backwards w.r.t. the direction of flow perturbations). Regarding the specific goal of acting at a shockfoot and the four aforementioned source terms [4], the authors of [9] demonstrate that the first two source terms (mass source at stagnation conditions, and normal force) may displace the shock and strongly alter near-field forces if located along the $\mathscr{C}^+$/ $\mathscr{C}^-$of the shock-foot whereas the fourth source (change in stagnation pressure at fixed static pressure and total enthalpy) may displace the shock-foot if located along the stagnation streamline or along the wall upwind the shock.
The demonstrated ODEs along the $\mathscr{S}$, $\mathscr{C}^-$and $\mathscr{C}^+$curves are hence consistent with known lines of specific influence on drag or lift of classical steady Eulerian flows. These lines also appear in the search of optimal forcings in control studies [21, 22] but we do not extend on this aspect due to the different base equations.

3.2. Consistency with the analytical adjoint field of 2D supersonic constant flow areas and the equations for the adjoint gradient at shocks

In reference [20] Todarello *et al.* derived the mathematical expression of the 2D Eulerian adjoint vector in a supersonic zone with constant flow (typically upwind the detached shockwave created by an airfoil). The angle of attack being α and Mach number M, this formula reads

$$\begin{aligned}\psi(x,y) &= \varphi_\alpha(x\,\sin(\alpha)-y\,\cos(\alpha))\lambda_0^\alpha+\varphi_{\alpha+\beta}(x\,\sin(\alpha+\beta)-y\,\cos(\alpha+\beta))\lambda_0^{\alpha+\beta}\\ &+ \varphi_{\alpha-\beta}(x\,\sin(\alpha-\beta)-y\,\cos(\alpha-\beta))\lambda_0^{\alpha-\beta},\end{aligned}\tag{31}$$

where $\beta=\sin^{-1}(1/M)$, φ_α, $\varphi_{\alpha-\beta}$, $\varphi_{\alpha-\beta}$ are three scalar functions, the λ_0^μ are left eigenvectors[9] of $A\sin(\mu)-B\cos(\mu)$

$$\lambda_0^{\alpha-\beta}=\begin{pmatrix}\frac{c}{\rho}\left(1+\frac{\gamma_1}{2}M^2\right)\\ \frac{1}{\rho}\left(\sin(\alpha-\beta)-\gamma_1\frac{u}{c}\right)\\ \frac{1}{\rho}\left(-\cos(\alpha-\beta)-\gamma_1\frac{v}{c}\right)\\ \frac{\gamma_1}{\rho c}\end{pmatrix},\quad \lambda_0^{\alpha+\beta}=\begin{pmatrix}\frac{c}{\rho}\left(1+\frac{\gamma_1}{2}M^2\right)\\ -\frac{1}{\rho}\left(\sin(\alpha+\beta)+\gamma_1\frac{u}{c}\right)\\ -\frac{1}{\rho}\left(-\cos(\alpha+\beta)+\gamma_1\frac{v}{c}\right)\\ \frac{\gamma_1}{\rho c}\end{pmatrix}\quad \lambda_0^{\alpha}=\begin{pmatrix}-1-\frac{\gamma_1}{2}M^2\\ \frac{\gamma_1 u}{c^2}+\frac{2\,\cos(\alpha)}{\cos(\alpha)u+\sin(\alpha)v}\\ \frac{\gamma_1 v}{c^2}+\frac{2\,\sin(\alpha)}{\cos(\alpha)u+\sin(\alpha)v}\\ -\frac{\gamma_1}{c^2}.\end{pmatrix}\tag{32}$$

which formulas [23] have been simplified here using the null eigenvalues relations valid in this specific context: $u\,\sin(\alpha)-v\,\cos(\alpha)=0$, $u\,\sin(\alpha-\beta)-v\,\cos(\alpha-\beta)+c=0$, $u\,\sin(\alpha+\beta)-v\,\cos(\alpha+\beta)-c=0$. Equation (31) is the mathematical formula for the three stripes field depicted in figure 2. Each φ scalar function expresses the combined variation in the amplitude of the adjoint components normally to the stripe direction. Each stripe is crossed by the characteristic lines oriented in the direction of the other two and we question whether equation (23), (24), (30) provide new information on the φ functions.
Considering the stripe oriented in the $\alpha-\beta$ direction, we first note that equation (30) with the t^- value, is automatically satisfied in its geometrical domain since $\varphi_{\alpha-\beta}(x\,\sin(\alpha-\beta)-y\,\cos(\alpha-\beta))\lambda_0^{\alpha-\beta}$ induces no variation of the ψ components in the $\mathscr{C}^-$direction. Regarding the conditions for satisfying (23) and (24) along an $\mathscr{S}$curve, and satisfying (30) along a $\mathscr{C}^+$curve where they cross the $\alpha-\beta$ stripe (as in fig. 2 right), we introduce the three functions

$$\begin{aligned}\Gamma_S^1(s) &= E_c\psi_1+Hu\psi_2+Hv\psi_3+H^2\psi_4\\ \Gamma_S^2(s) &= \psi_1+u\psi_2+v\psi_3+E_c\psi_4\\ \Gamma_{C+}(s) &= (u+vt^+)\psi_1+(u^2+v^2)(\psi_2+t^+\psi_3)+H(u+vt^+)\psi_4,\end{aligned}$$

with s the curvilinear abscissa along the curve mentioned in the index. It is proven in appendix D that

$$\frac{d\Gamma_S^1}{ds}=0 \qquad \frac{d\Gamma_S^2}{ds}=0 \qquad \frac{d\Gamma_{C+}}{ds}=0$$

without condition on the φ functions. As the flow is constant, this is equivalent to the satisfaction of the ODEs along the $\mathscr{S}$ and the $\mathscr{C}^+$curves. The other possible crossing of the stripes and the curves also do not provide conditions on the φ functions. We hence have not gained information on the analytical adjoint field of 2D supersonic constant flow zones but this automatic consistency establishes a link, via a series the orthogonality properties, between the coefficients of the differential equation (23), (24), (30) and the relevant left eigenvectors of the Euler flux Jacobian (32).

Regarding shock-waves, it is know that, for classical QoIs like pressure integrals at the wall, the adjoint vector is continuous at shocks although the flow is not, whereas the adjoint gradient may be discontinuous. In most common cases, although a shockwave only makes the normal component of the velocity subsonic, the $\mathscr{C}^+$and $\mathscr{C}^-$curves end at the shock and the most interesting discussion regards the consequences of (23), (24). As they are valid both sides of the shock, the jump operator may be applied to them across the discontinuity Σ:

$$[\![E_c\,\frac{d\psi_1}{ds}+H(u\,\frac{d\psi_2}{ds}+v\,\frac{d\psi_3}{ds})+\,H^2\frac{d\psi_4}{ds}]\!]=0 \qquad [\![\frac{d\psi_1}{ds}+u\,\frac{d\psi_2}{ds}+v\,\frac{d\psi_3}{ds}+E_c\frac{d\psi_4}{ds}]\!]=0,$$

where all terms but H may be discontinuous. Unfortunately, it does not seem possible to reduce these equations to the simpler ones for the adjoint gradient discontinuity [8, 9] where the derivatives in the two directions of the local frame of reference attached to the shock appear independently. Conversely, we note that in the case of a normal shock, the equations derived in [8] prove the previous two jump equations.

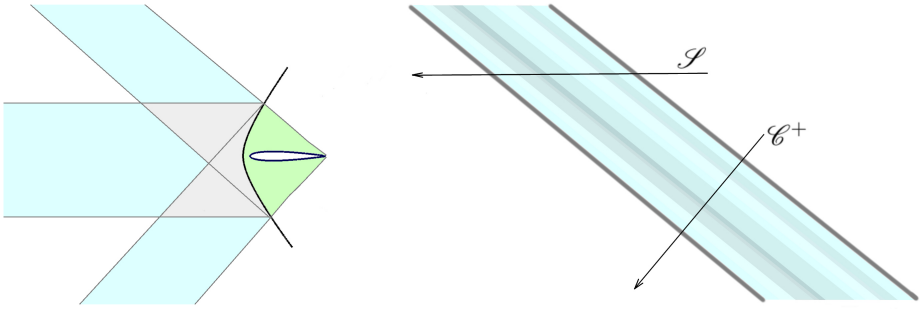

Figure 2: Left: Sketch of lift/drag adjoint field for a supersonic flow about an airfoil. Individual stripes (blue) and superimposition of the three stripes (grey) in the constant flow zone ; nonzero adjoint zone downwind the shockwave (green). Right: $\mathscr{C}^-$stripe crossed by a $\mathscr{S}$and a $\mathscr{C}^+$curve

3.3. Numerical assessment method

The numerical assessment method consists in computing flow and adjoint fields over a very fine mesh, and calculating the following integrals:

$$K_O S^1 = \int_{\mathscr{S}}\left(E_c\,\frac{d\psi_1}{ds}+H(u\,\frac{d\psi_2}{ds}+v\,\frac{d\psi_3}{ds})+\,H^2\frac{d\psi_4}{ds}\right)ds \tag{33}$$

$$K_O S^2 = \int_{\mathscr{S}}\left(\frac{d\psi_1}{ds}+u\,\frac{d\psi_2}{ds}+v\,\frac{d\psi_3}{ds}+\,E_c\frac{d\psi_4}{ds}\right)ds \tag{34}$$

$$K_O C^+ = \int_{\mathscr{C}^+}\left((u+vt^+)\,\frac{d\psi_1}{ds}+(u^2+v^2)(\frac{d\psi_2}{ds}+t^+\frac{d\psi_3}{ds})+H(u+vt^+)\,\frac{d\psi_4}{ds}\right)ds \tag{35}$$

$$K_O C^- = \int_{\mathscr{C}^-}\left((u+vt^-)\,\frac{d\psi_1}{ds}+(u^2+v^2)(\frac{d\psi_2}{ds}+t^-\frac{d\psi_3}{ds})+H(u+vt^-)\,\frac{d\psi_4}{ds}\right)ds. \tag{36}$$

Here the intermediate subscript O stands for the output functional of interest ; it is subsequently replaced by L (for the lift, CLp) and D (for drag, CDp, consistently with the adjoint vector placed on the right-hand side.

The integration is performed in the forward sense for the adjoint, that is, backwards w.r.t. the direction of the flow information propagation. The integration domain for the above line integrals extends to the interior of the disk of radius $3c$ centred at $(0.5c, 0)$, chosen for plotting readability, while the flow computational domain itself extends to $150c$. It may be shorter, in particular in the transonic case where the $\mathscr{C}^+$and $\mathscr{C}^-$curves are limited to the supersonic bubble(s). The four quantities $K_O S^1$,..., $K_O C^-$ are expected to be close to zero and, to avoid any error in scale, also calculated and plotted are the corresponding subparts, that is, for $K_O S^1$ for example,

$$K_O S_1^1 = \int_{\mathscr{S}} \left(E_c \, \frac{d\psi_1}{ds} \right) ds \qquad K_O S_2^1 = \int_{\mathscr{S}} \left(Hu \, \frac{d\psi_2}{ds} \right) ds$$

$$K_O S_3^1 = \int_{\mathscr{S}} \left(Hv \, \frac{d\psi_3}{ds} \right) ds \qquad K_O S_4^1 = \int_{\mathscr{S}} \left(H^2 \frac{d\psi_4}{ds} \right) ds.$$

The sum of the four terms is expected to be much smaller than each one of them individually. All the integrals are calculated backwards, along a finely discretized characteristic curve, simply by the trapezoidal rule.

The discrete flows and adjoints were available from former computations [9] in which the Jameson-Schmidt-Turkel scheme [24] was applied, and using the discrete adjoint module of the *elsA* code [25, 26]. Of course when trying to assess properties of exact adjoint fields from numerical discrete solutions, it is desirable to work either with continuous adjoints or with dual consistent discrete adjoints[27, 28, 29]. Precisely in [9], it was demonstrated for structured meshes how to slightly modify the scheme's Jacobian (in the derivative of the dissipation flux, for the next to wall faces) to get a dual consistent linearization. This slight modification of the exact scheme Jacobian is retained here to work with adjoint fields that are consistent with the continuous equations discussed in §2. Note also that these adjoint fields have also been satisfactorily verified by a posteriori discretization of the continuous adjoint equation[9].

Only the solutions calculated over the finest mesh defined in reference [30] (structured 4097×4097 mesh) are used here. The iso-Mach number lines, iso-first component of CLp adjoint and the extracted curves may be seen for all cases in figure 3.

3.4. Numerical assessment of the ODEs for a supersonic flow about the NACA0012 airfoil

The retained flow conditions are $M_\infty = 1.5$, $\alpha = 1^o$. We first assess the streamtraces equations (23) (24). The $K_D S^1$, $K_D S^2$, $K_L S^1$, $K_L S^2$ integrals and their subparts are calculated along the trajectory passing through $(c, 0.1c)$. The integration indeed leads to very small values of $K_D S^1$, $K_D S^2$, $K_L S^1$, $K_L S^2$ along the curve w.r.t. their subparts. It is well-known for this of kind of flow that the exact lift- and drag- adjoint is equal to zero downstream the backwards flow-characteristics emanating from the trailing edge (since no perturbation downstream those two lines can affect the pressure on the aerofoil and, consequently, the lift or the drag – see for example fig. 6 and A21 in [9]). This property is well satisfied by discrete adjoint fields and, as the integration is performed backwards along the streamtrace, null values of $K_D S^1$, $K_D S^2$, $K_L S^1$, $K_L S^2$ and all their subparts are observed above a specific x corresponding to the intersection of the streamtrace with this trailing-edge $\mathscr{C}^-$. The integration of (23) and (24) reveals (i) the discontinuity of the integration variables (the adjoint components) at $x \simeq 0.85$ that appears as a discontinuity in the subpart curves ; (ii) a discontinuity of the integration coefficients, when crossing the detached shock wave at $x \simeq -0.08$, that results in strong gradients in the subparts curves. None of those discontinuities alters the almost null values of $K_D S^1$ $K_D S^2$, $K_D L^1$ and $K_L S^2$. The strong adjoint gradients in the subsonic bubble (approximately $x \in [-0.08, 0.05]$) also clearly translate the K_S curves. Finally, note that for x lower than $\simeq -0.05$ the flow is constant (so the streamtrace is a straight line) and for x lower than $\simeq -1$ the backward streamtrace enters a zone of constant adjoint along its direction (see fig. 2 left and equation (31)). This theoretical property is well translated in constant sections of the curves. The results are equivalently accurate for lift and drag. They are presented for the drag in figure 4.

A $\mathscr{C}^+$and a $\mathscr{C}^-$curve are then extracted using equation (4). The selected $\mathscr{C}^+$is initiated at $x \simeq 0.3$ upper side and the retained $\mathscr{C}^-$starts at the same abscissa but on the lower side. This choice was guided by the extraction method and the observation that k^+ (resp. k^-) is almost constant on the lower (resp. upper) side. The $K_D C^+$, $K_L C^+$, $K_D C^-$,$K_L C^-$ terms and their subparts have been computed. The results appear to be very satisfactory. Also observed is the equality of $K_D C_1^+$ and $K_D C_4^+$, $K_L C_1^+$ and $K_L C_4^+$ and along the $\mathscr{C}^+$and correspondingly along the $\mathscr{C}^-$curves. This is due to the fact that $\psi_1 = H\psi_4$ (for Euler flows and for pressure-based integrals along the wall that is well satisfied at the discrete

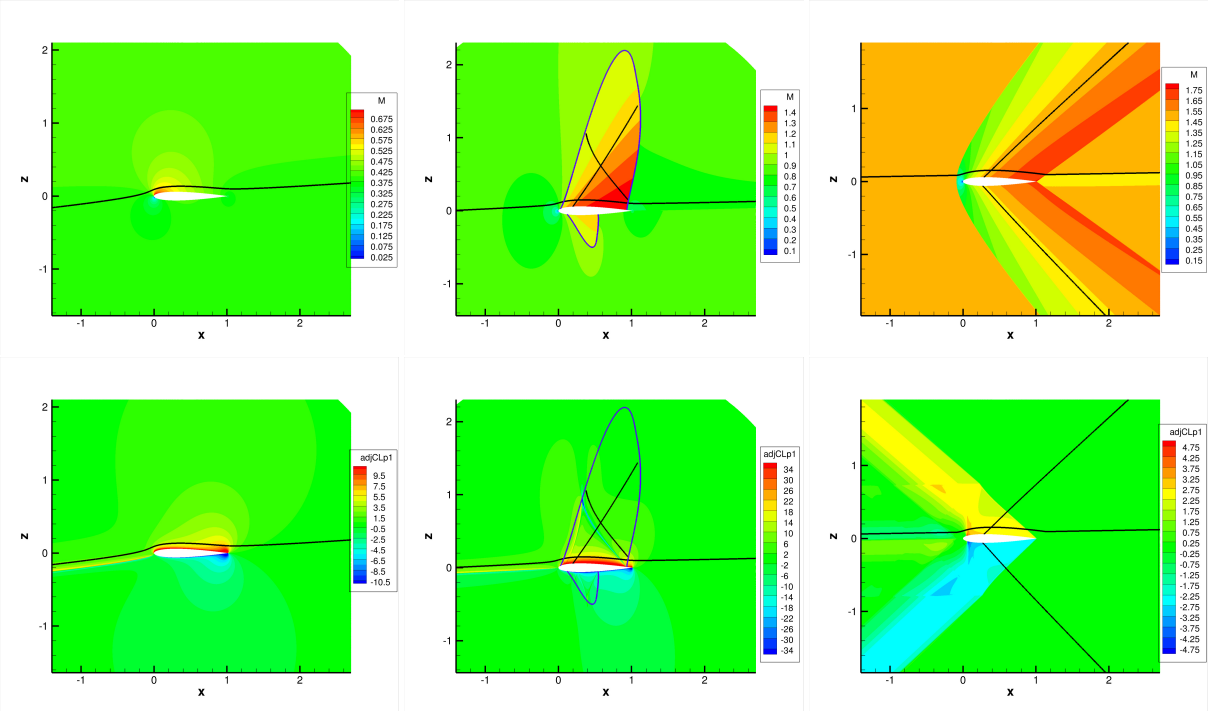

Figure 3: Simulations over the 4097×4097 mesh of [30]. iso-Mach number lines (upper three plots) and iso-ψ^1_{CLp} lines (lower three plots) and extracted curves. Left, subsonic case: streamline. Middle, transonic case: streamline, $\mathscr{C}^+$, $\mathscr{C}^-$(black) and sonic line (violet). Right supersonic case: streamline, $\mathscr{C}^+$(upper side), $\mathscr{C}^-$(lower side)

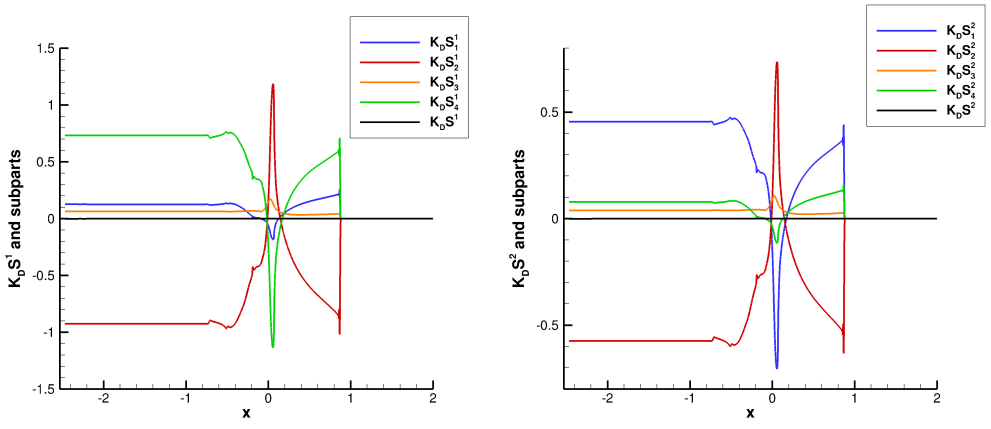

Figure 4: $M_\infty = 1.50$, $\alpha = 1^o$, (4097×4097 mesh [30]) Numerical assessment of equation (23) (left) and (24) (right) for the lift. Method of verification: the black curve should ideally coincide with the x axis

level – see for example [9] fig. A21, A22, A23) and to the expression of the $d\psi_1$ and $d\psi_4$ terms in (29). Figure 5 presents the verification plots for the two functions along the selected $\mathscr{C}^+$.

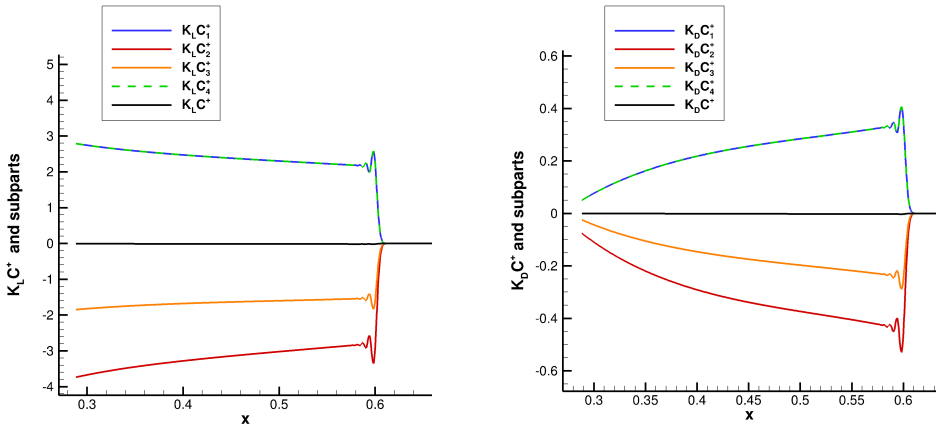

Figure 5: $M_\infty = 1.50$, $\alpha = 1^o$, (4097×4097 mesh [30]) Numerical assessment of equation (29) for the lift (left) and for the drag (right). Method of verification: the black curve should ideally coincide with the x axis

3.5. Numerical assessment of the ODEs for a transonic flow about the NACA0012 airfoil

The flow conditions are $M_\infty = 0.85$, $\alpha = 2^o$. Careful verification of the streamstraces equations (23) (24) has been performed for the streamtrace passing through $(c, 0.1c)$ and very satisfactory results have been found. As in the previous section, the intersection of the $\mathscr{S}$curve with the shockwave results in the subsparts curves in very strong gradients but does not affect the almost null value of $K_D S^1$, $K_D S^2$, $K_L S^1$, $K_L S^2$. As similar results have been presented in the previous and the next subsections, we focus here on the $\mathscr{C}^+$and $\mathscr{C}^-$curves. A $\mathscr{C}^+$and a $\mathscr{C}^-$curves have been extracted taking care to select the longest possible curves (and to avoid, for the $\mathscr{C}^-$the curve passing by the shock-foot where numerical divergence of the adjoint may be observed). The selected $\mathscr{C}^+$(resp. $\mathscr{C}^-$) is passing approximately through the point $(0.197, 0.057)$ (resp. $(0.954, 0141)$). The verification of the consistency of the numerical solutions w.r.t. (29) is satisfactory although the largest observed errors appear in this case, for the $\mathscr{C}^-$curve, for the lift, in the vicinity of the inlet of the supersonic bubble – see figure 6. This largest observed error is about 2% of the largest absolute value of the four subparts. The integrals along the $\mathscr{C}^-$are regular, whereas those along the $\mathscr{C}^+$exhibit a sharp peak close to $x \simeq 0.52$, at the intersection with the $\mathscr{C}^-$passing by the shockfoot. We refer to §3.1 for the reason of the corresponding strong adjoint gradient.

3.6. Numerical assessment of the streamtrace ODEs for a subsonic flow about the NACA0012 airfoil

We expect relations (23) and (24) to be valid along the trajectories of a subsonic flow. The retained flow conditions have been $M_\infty = 0.4$, $\alpha = 5^o$. The $K_D S^1$, $K_D S^2$, $K_L S^1$, $K_L S^2$ integrals and their subparts are calculated along the trajectory passing through $(c, 0.1c)$. The integration indeed leads to very small values of $K_D S^1$, $K_D S^2$, $K_L S^1$, $K_L S^2$ along the curve w.r.t. their subparts. The results are equivalently good for lift and drag and are presented in figure 7 for the lift. The lower left plot of figure 3 presents the typical aspect of subsonic lift or drag adjoints indicating that an actuation able to significantly alter these QoIs is to be applied in the immediate vicinity of the wall. This property translates in weakly varying curves far from the profile in our verification plots for this test case.

4. Conclusion

Ordinary Differential Equations have been derived for the adjoint Euler equations using in a first step the method of characteristics in 2D. The differential equations satisfied along the streamtraces in 2D have then been extended to 3D and the combination of equations method used for the derivation in this case also provides a simpler proof of

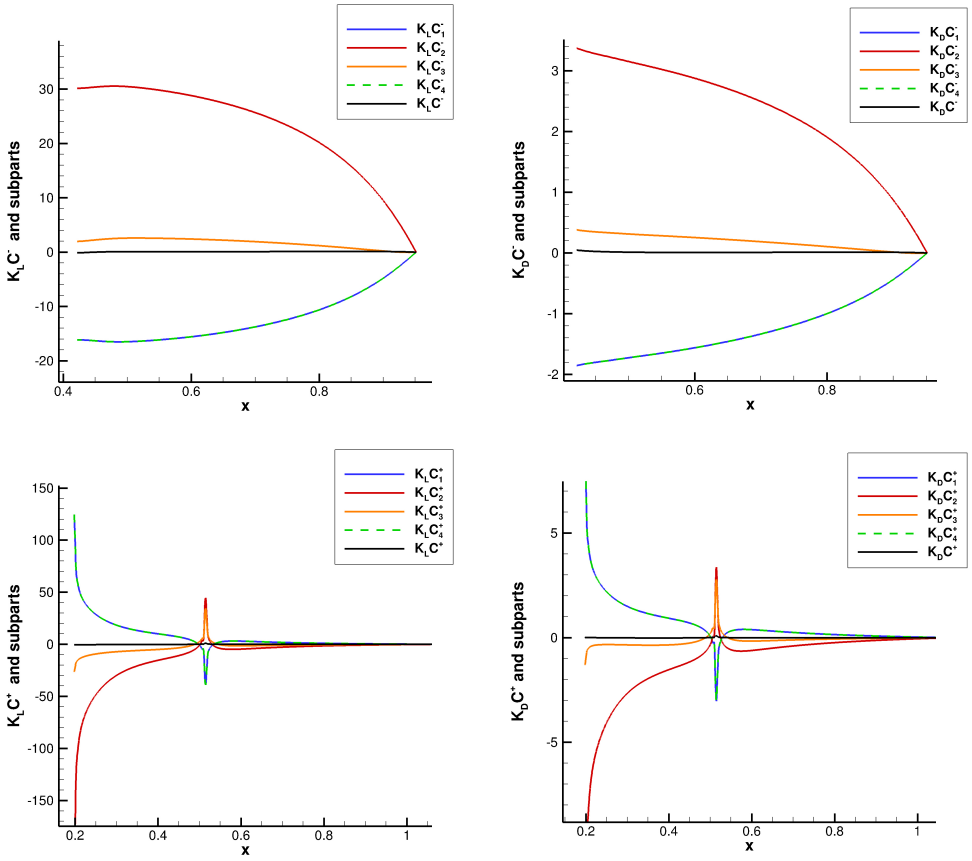

Figure 6: $M_\infty = 0.85$, $\alpha = 2^o$, (4097×4097 mesh [30]) Numerical assessment of equation (29) for the lift (left) and for the drag (right), for the selected $\mathscr{C}^-$(up) and $\mathscr{C}^-$(down). Method of verification: the black curve should ideally coincide with the x axis

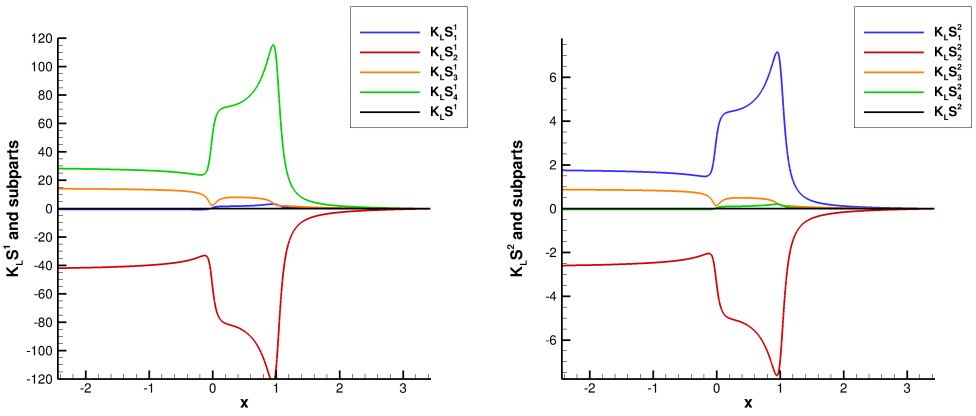

Figure 7: $M_\infty = .40$, $\alpha = 5^o$, (4097×4097 mesh [30]) Numerical assessment of equation (23) (left) and (24) (right) for the lift. Method of verification: black curve should ideally coincide with the x axis

the corresponding 2D equations. All these ODEs are non linear differential equations that cannot be integrated for non-constant flows.
The adjoint vector expresses the sensitivity of its corresponding scalar QoI to a local perturbation in the flow equations. Its variations in the fluid domain are often difficult to analyse as it precisely avoids the calculation of the flow perturbation that causes the change in the QoI. Nevertheless lift and drag adjoint fields have been examined since a long time, and the presented equations for 2D problems clarify their highest values and the strong sensitivity of their associated QoIs to perturbations located along specific lines [19, 20, 8, 9].
These findings have been illustrated with flows, lift-adjoints, and drag-adjoints over the classical NACA0012 airfoil using a very fine mesh and a dual-consistent adjoint method. The conducted tests lead to very satisfactory results (although minor deviations in our transonic case close to the inlet of the upper side supersonic bubble). The demonstrated equations (23),(24), and (30) hence also provide a verification tool for discrete adjoint fields.

SUPPLEMENTARY MATERIAL

Supplementary material consists of:
– five python scripts allowing to check the algebraic expressions of the C^l_{mx} and C^l_{my} coefficients w.r.t. their definition as determinants and one python script allowing the numerical verification of the results of IIIB ;
– six outputs of Maple scripts checking the rank of the sets of differential forms satisfied along the streamtraces, $\mathscr{C}^+$, and $\mathscr{C}^-$.

ACKNOWLEDGMENTS

The authors express their warm gratitude to J.C. Vassberg and A. Jameson for allowing the co-workers of D. Destarac to use their hierarchy of O-grids around the NACA0012 airfoil, as well as E. Hubert and B. Mourrain (Inria Aromath Project Team) for their helpful guidance for the analytical developments using the computer algebra software Maple. The authors also thank Florent Renac, Fulvio Sartor and Martin Duguey for many fruitful discussions.

This research did not receive any specific grant from funding agencies in the public, commercial or not-for-profit sector.

DATA AVAILABILITY

The data consists of the three flow-fields about the NACA0012 airfoil and the corresponding lift-adjoint and drag-adjoint. They are available as Tecplot binary or formatted files from the corresponding author.

AUTHOR CONTRIBUTIONS

Jacques Peter: Investigation (lead); Methodology (lead); Validation (equal); Writing original draft (lead). Jean-Antoine Désidéri: Investigation (supporting); Methodology (supporting); Validation (equal); Writing original draft (supporting); Writing review and editing.

A. Calculation and expressions of the C^k_{ij} coefficients

Two or three of the vectors $(-B_1+tA_1)$, $(-B_2+tA_2)$, $(-B_3+tA_3)$ and $(-B_4+tA_4)$ appear in the formulas of the C^k_{ij} coefficients expressed as the determinant of a 4×4 matrix. They may be precalculated as

$$-B_1+tA_1=\begin{bmatrix}0\\ t\\ -1\\ 0\end{bmatrix} \qquad -B_2+tA_2=\begin{bmatrix}t\ \gamma_1\ E_c-u\kappa\\ -v+t(3-\gamma)u\\ -u-t\gamma_1 v\\ t\gamma_1\end{bmatrix}$$

$$-B_3+tA_3=\begin{bmatrix}-\gamma_1\ E_c-v\kappa\\ \gamma_1 u+tv\\ -(3-\gamma)v+tu\\ -\gamma_1\end{bmatrix} \qquad -B_4+tA_4=\begin{bmatrix}(\gamma_1\ E_c-H)\kappa\\ tH-\gamma_1 u\kappa\\ -H-\gamma_1 v\kappa\\ \gamma\kappa\end{bmatrix}$$

The expressions of the $C^l_{1x}, C^l_{2x}, C^l_{3x}, C^l_{1y}, C^l_{2y}, C^l_{3y}, C^l_{4y}$ are gathered below (the C^l_{4x} being given in §2.2). We recall that, with our notations, the null differential form along the $\mathscr{S}$, $\mathscr{C}^-$and $\mathscr{C}^+$derived from the existence of, e.g. $(\partial\psi_i/\partial y)$, reads $C^1_{iy}d\psi_1 - C^2_{iy}d\psi_2 + C^3_{iy}d\psi_3 - C^4_{iy}d\psi_4 = 0$

• The coefficients C^l_{1x} are expressed below

$$\begin{aligned}
C^1_{1x} &= -dx^3\ \kappa\ ((2tu+(t^2-1)v)(\gamma_1 H+\gamma_1 E_c+\gamma v\kappa)-(u+vt)(\gamma_1 tH+\gamma_1 u\kappa+\gamma v\kappa t))\\
C^2_{1x} &= dx^2dy\ \gamma_1\ \kappa\ (u^2+v^2)\ H\\
C^3_{1x} &= -dx^2dy\ \gamma_1\ \kappa\ t\ (u^2+v^2)\ H\\
C^4_{1x} &= dx^2dy\ \gamma_1\ \kappa\ (u+vt)\ H^2
\end{aligned}$$

• The coefficients C^l_{2x} are expressed below

$$\begin{aligned}
C^1_{2x} &= -dx^2dy\ \kappa\ (\gamma_1 H+\gamma_1 E_c+\gamma v\kappa)\\
C^2_{2x} &= -dx^3\ \kappa\ (\gamma_1 u^2v-uv^2t+\gamma v^3-\gamma_1(ut+v)(E_c+H))\\
C^3_{2x} &= dx^2dy\ \kappa\ (\gamma_1 u^2v-uv^2t+\gamma v^3-\gamma_1(ut+v)(E_c+H))\\
C^4_{2x} &= dx^2dy\ H\ \kappa\ (\gamma_1 H+\gamma_1 E_c+\gamma v\kappa)
\end{aligned}$$

• The coefficients C^l_{3x} are expressed below

$$\begin{aligned}
C^1_{3x} &= dx^2dy\ \kappa\ (t\gamma_1 H+t\gamma_1 E_c-\gamma u\kappa)\\
C^2_{3x} &= -dx^2dy\ \kappa\ ((\gamma+1)u^2v-t\gamma_1 uv^2+(v+ut)(\gamma_1 E_c+\gamma_1 H-\gamma u^2))\\
C^3_{3x} &= dx^3\ \kappa\ ((tv^2-u\kappa)(-\gamma_1 u+(\gamma+1)tv)-(ut-(1+2t^2)v)(\gamma_1 E_c+\gamma_1 H-\gamma v^2))\\
C^4_{3x} &= -dx^2dy\ H\ \kappa\ (t\gamma_1 H+t\gamma_1 E_c-\gamma u\kappa)
\end{aligned}$$

• The coefficients C^l_{1y} are expressed below

$$\begin{aligned}
C^1_{1y} &= dx^3\ \kappa\ \left((\gamma_1+\gamma t^2)u^3-2u^2vt-\gamma_1 t\kappa H+(\gamma+\gamma_1 t^2)uv^2-\gamma_1 u\ (1+t^2)\ E_c\right)\\
C^2_{1y} &= -dx^3\gamma_1\ \kappa\ (u^2+v^2)\ H\\
C^3_{1y} &= dx^3\ \gamma_1\ t\ \kappa\ (u^2+v^2)\ H\\
C^4_{1y} &= -dx^3\ \gamma_1\ \kappa\ (u+vt)\ H^2
\end{aligned}$$

• The coefficients C^l_{2y} are expressed below

$$\begin{aligned}
C^1_{2y} &= dx^3\ \kappa\ (\gamma_1 H+\gamma_1 E_c+\gamma v\kappa)\\
C^2_{2y} &= -dx^3\ \kappa\ ((v\kappa+u^2)(vt-(\gamma_1+\gamma t^2)u)-(vt-(2+t^2)u))(\gamma_1 E_c+\gamma_1 H+\gamma v\kappa))\\
C^3_{2y} &= -dx^3\ \kappa\ (\gamma_1 u^2v-uv^2t+\gamma v^3-\gamma_1(ut+v)(E_c+H))\\
C^4_{2y} &= -dx^3\ H\ \kappa\ (\gamma_1 H+\gamma_1 E_c+\gamma v\kappa)
\end{aligned}$$

• The coefficients C^l_{3y} are expressed below

$$\begin{aligned}
C^1_{3y} &= -dx^3\ \kappa\ (\gamma_1 tE_c+\gamma_1 tH-\gamma u\kappa)\\
C^2_{3y} &= dx^3\ \kappa\ ((\gamma+1)u^2v-t\gamma_1 uv^2+(v+ut)(\gamma_1 E_c+\gamma_1 H-\gamma u^2))\\
C^3_{3y} &= -dx^3t\kappa((\gamma+1)u^2v-t\gamma_1 uv^2+(v+ut)(\gamma_1 E_c+\gamma_1 H-\gamma u^2))\\
C^4_{3y} &= dx^3\kappa\ H\ (\gamma_1 tE_c+\gamma_1 tH-\gamma u\kappa)
\end{aligned}$$

• The coefficients C^l_{4y} are expressed below

$$\begin{aligned}
C^1_{4y} &= -dx^3\ \gamma_1\ \kappa\ (u+vt)\\
C^2_{4y} &= dx^3\ \gamma_1\ \kappa\ (u^2+v^2)\\
C^3_{4y} &= -dx^3\ \gamma_1\ \kappa\, t\ (u^2+v^2)\\
C^4_{4y} &= dx^3\kappa\left((\gamma_1+\gamma t^2)u^3-2u^2vt-\gamma_1 t\,\kappa H+(\gamma+\gamma_1 t^2)uv^2-\gamma_1 u\ (1+t^2)\ E_c\right)
\end{aligned}$$

B. General properties of the C^l_{mx} and C^l_{my} coefficients

Equation (6) refers to the limit of small space steps and the search of characteristic curves ; nevertheless, the expressions of the C^l_{mx} and C^l_{my} coefficients may be considered for an arbitrary direction and an arbitrary norm of vector (dx,dy). Without any assumption linking (dx,dy) and (u,v), the relations between the coefficients of the same differential forms are:

$$C^4_{1x} = HC^1_{1x} \quad C^3_{1x}=tC^2_{1x}\ ;\ C^4_{2x}=-HC^1_{2x} \quad C^3_{2x}=-tC^2_{2x}\ ;\ C^4_{3x}=-HC^1_{3x}\ ;\ C^3_{4x}=-tC^2_{4x} \tag{37}$$

$$C^4_{1y} = HC^1_{1y} \quad C^3_{1y}=tC^2_{1y}\ ;\ C^4_{2y}=-HC^1_{2y}\ ;\ C^4_{3y}=-HC^1_{3y} \quad C^3_{3y}=-tC^2_{3y}\ ;\ C^3_{4y}=-tC^2_{4y} \tag{38}$$

Besides, twelve of the sixteen coefficients of the differential forms for the x and y derivatives are proportional by a $(-t)$ factor:

$$C^2_{1x} = -t\ C^2_{1y} \qquad C^3_{1x}=-t\ C^3_{1y} \qquad C^4_{1x}=-t\ C^4_{1y} \tag{39}$$

$$C^1_{2x} = -t\ C^1_{2y} \qquad C^3_{2x}=-t\ C^3_{2y} \qquad C^4_{2x}=-t\ C^4_{2y} \tag{40}$$

$$C^1_{3x} = -t\ C^1_{3y} \qquad C^2_{3x}=-t\ C^2_{3y} \qquad C^4_{3x}=-t\ C^4_{3y} \tag{41}$$

$$C^1_{4x} = -t\ C^1_{4y} \qquad C^2_{4x}=-t\ C^2_{4y} \qquad C^3_{4x}=-t\ C^3_{4y} \tag{42}$$

Finally, the C^1_{1l} and C^4_{4l} coefficients are equal

$$C^1_{1x}=C^4_{4x} \qquad\qquad C^1_{1y}=C^4_{4y} \tag{43}$$

C. Streamstrace ODEs in dimension 3

From 2D equations (23) and (24), we can infer corresponding candidate equations for the adjoint vector along the streamtraces in 3D:

$$E_c\ \frac{d\psi_1}{ds}+H(u\ \frac{d\psi_2}{ds}+v\ \frac{d\psi_3}{ds}+w\ \frac{d\psi_4}{ds})+\ H^2\frac{d\psi_5}{ds}=0 \tag{44}$$

$$\frac{d\psi_1}{ds}+u\ \frac{d\psi_2}{ds}+v\ \frac{d\psi_3}{ds}+w\ \frac{d\psi_4}{ds}+E_c\frac{d\psi_5}{ds}=0. \tag{45}$$

Could these equations be possibly proven from the 3D Euler adjoint equations

$$-A^T\frac{\partial\psi}{\partial x}-B^T\frac{\partial\psi}{\partial y}-C^T\frac{\partial\psi}{\partial z}=0, \tag{46}$$

where the 3D transposed Jacobian of Euler fluxes read

$$A^T=\begin{bmatrix}0 & (\gamma_1E_c-u^2) & -uv & -uw & (\gamma_1E_c-H)u\\ 1 & -\gamma_1u+2u & v & w & (H-\gamma_1u^2)\\ 0 & -\gamma_1v & u & 0 & -\gamma_1uv\\ 0 & -\gamma_1w & 0 & u & -\gamma_1uw\\ 0 & \gamma_1 & 0 & 0 & \gamma u\end{bmatrix} \qquad B^T=\begin{bmatrix}0 & -uv & (\gamma_1E_c-v^2) & -vw & (\gamma_1E_c-H)v\\ 0 & v & -\gamma_1u & 0 & -\gamma_1uv\\ 1 & u & -\gamma_1v+2v & w & (H-\gamma_1v^2)\\ 0 & 0 & -\gamma_1w & v & -\gamma_1vw\\ 0 & 0 & \gamma_1 & 0 & \gamma v\end{bmatrix}$$

$$C^T = \begin{bmatrix} 0 & -uw & -vw & (\gamma_1 E_c - w^2) & (\gamma_1 E_c - H)w \\ 0 & w & 0 & -\gamma_1 u & -\gamma_1 uw \\ 0 & 0 & w & -\gamma_1 v & -\gamma_1 vw \\ 1 & u & v & -\gamma_1 w + 2w & (H - \gamma_1 w^2) \\ 0 & 0 & 0 & \gamma_1 & \gamma W \end{bmatrix}$$

s being the curvilinear abscissa along a trajectory in the direction opposite to the flow displacement, the differentiation w.r.t. s may be expressed as

$$\frac{d}{ds} = -\frac{u}{\|U\|}\frac{d}{dx} - \frac{v}{\|U\|}\frac{d}{dy} - \frac{w}{\|U\|}\frac{d}{dz}$$

First considering (45), the equation with the simpler coefficients, this equation is satisfied in the fluid domain if and only if

$$\begin{aligned} &(u\frac{d\psi_1}{dx} + v\frac{d\psi_1}{dy} + w\frac{d\psi_1}{dz}) + u(u\frac{d\psi_2}{dx} + v\frac{d\psi_2}{dy} + w\frac{d\psi_2}{dz}) \\ +v(u\frac{d\psi_3}{dx} + v\frac{d\psi_3}{dy} + w\frac{d\psi_3}{dz}) &+ w(u\frac{d\psi_4}{dx} + v\frac{d\psi_4}{dy} + w\frac{d\psi_4}{dz}) \\ &+E_c(u\frac{d\psi_5}{dx} + v\frac{d\psi_5}{dy} + w\frac{d\psi_5}{dz}) = 0 \end{aligned} \tag{47}$$

(where we have removed the norm of the velocity and the minus sign thanks to the homogeneity of the equation). We now search if a combination of the lines of (46) that would result in (47). For the required ψ_1 terms to appear, the combination $(-uL_2 - vL_3 - wL_4)$ (L_j denoting the j-th line of (46)) needs to be calculated:

$$\begin{aligned} [u \quad & (-2\gamma_1 E_c + 2u^2) \quad 2uv \quad & & 2uw \quad (Hu - 2\gamma_1 uE_c)]\frac{\partial\psi}{\partial x} \\ +[v \quad & 2uv \quad & (-2\gamma_1 E_c + 2v^2) \quad & 2vw \quad (Hv - 2\gamma_1 vE_c)]\frac{\partial\psi}{\partial y} \\ +[w \quad & 2uw \quad & 2vw \quad & (-2\gamma_1 E_c + 2w^2) \quad (Hw - 2\gamma_1 wE_c)]\frac{\partial\psi}{\partial z} = 0 \end{aligned}$$

Subtracting the first line, calculating $(-L_1 - uL_2 - vL_3 - wL_4)$, almost fixes the expected coefficients for the ψ_1 to ψ_4 derivatives:

$$\begin{aligned} [u \quad & (-\gamma_1 E_c + u^2) \quad uv \quad & & uw \quad -\gamma_1 uE_c]\frac{\partial\psi}{\partial x} \\ +[v \quad & uv \quad & (-\gamma_1 E_c + v^2) \quad & vw \quad -\gamma_1 vE_c]\frac{\partial\psi}{\partial y} \\ +[w \quad & uw \quad & vw \quad & (-\gamma_1 E_c + w^2) \quad -\gamma_1 wE_c]\frac{\partial\psi}{\partial z} = 0 \end{aligned}$$

Finally forming $(-L_1 - uL_2 - vL_3 - wL_4 - E_cL_5)$ yields

$$\begin{aligned} [u \quad & u^2 \quad uv \quad uw \quad uE_c]\frac{\partial\psi}{\partial x} \\ +[v \quad & uv \quad v^2 \quad vw \quad vE_c]\frac{\partial\psi}{\partial y} \\ +[w \quad & uw \quad vw \quad w^2 \quad wE_c]\frac{\partial\psi}{\partial z} = 0 \end{aligned}$$

that is exactly equation (47).
In order to demonstrate (44), we first form the combination $-((2E_c - H)L_1 + uE_cL_2 + vE_cL_3 + wE_cL_4)$ of the lines of the 3D adjoint Euler equations. This results in

$$
\begin{aligned}
&[uE_c \quad (u^2H-\gamma_1 HE_c) \quad uvH \quad uw \quad -\gamma HuE_c+H^2u]\frac{\partial\psi}{\partial x}\\
+&[vE_c \quad uvH \quad (v^2H-\gamma_1 HE_c) \quad vw \quad -\gamma HvE_c+H^2v]\frac{\partial\psi}{\partial y}\\
+&[wE_c \quad uwH \quad vwH \quad (w^2H-\gamma_1 HE_c) \quad -\gamma HwE_c+H^2w]\frac{\partial\psi}{\partial z}=0
\end{aligned}
$$

Adding $-E_c\ H\ L_5$ yields

$$
\begin{aligned}
&[uE_c \quad u^2H \quad uvH \quad uwH \quad H^2u]\frac{\partial\psi}{\partial x}\\
+&[vE_c \quad uvH \quad v^2H \quad vwH \quad H^2v]\frac{\partial\psi}{\partial y}\\
+&[wE_c \quad uwH \quad vwH \quad w^2H \quad H^2w]\frac{\partial\psi}{\partial z}=0
\end{aligned}
$$

that is equivalent to (44).

D. Demonstration of the properties presented in §3.2

The differentiation of the functions Γ_S^1, Γ_S^2 and Γ_{C+} appearing in section §3.2 uses the expression of the adjoint field where the $(\alpha-\beta)$-oriented stripe is non superimposed with the two other:

$$\psi(x,y)=\varphi_{\alpha-\beta}(x\ \sin(\alpha-\beta)-y\ \cos(\alpha-\beta))\lambda_0^{\alpha-\beta}$$

$$
\begin{aligned}
\frac{d\Gamma_S^1}{ds} &= E_c\frac{d\psi_1}{ds}+Hu\frac{d\psi_2}{ds}+Hv\frac{d\psi_3}{ds}+H^2\frac{d\psi_4}{ds}\\
\frac{d\Gamma_S^1}{ds} &= \left(E_c(\frac{c}{\rho}(1+\frac{\gamma_1}{2}M^2))+Hu(\frac{1}{\rho}(\sin(\alpha-\beta)-\gamma_1\frac{u}{c}))+Hv(\frac{1}{\rho}(-\cos(\alpha-\beta)-\gamma_1\frac{v}{c}))+H^2(\frac{\gamma_1}{\rho c})\right)\frac{d\varphi_{\alpha-\beta}}{d\xi}\frac{d\xi}{ds}\\
\frac{d\Gamma_S}{ds} &= \left(\frac{\gamma_1E_c}{\rho c}+\frac{c^2u}{\gamma_1\rho}\sin(\alpha-\beta)-\frac{c^2v}{\gamma_1\rho}\cos(\alpha-\beta)-\frac{\gamma_1Hu^2}{\rho c}-\frac{\gamma_1Hv^2}{\rho c}+\frac{H^2\gamma_1}{\rho c}\right)\frac{d\varphi_{\alpha-\beta}}{d\xi}\frac{d\xi}{ds}\\
&\quad(\quad \text{using}\quad u\ \sin(\alpha-\beta)-v\ \cos(\alpha-\beta)+c=0\quad\text{and}\quad H=E_c+C^2/\gamma_1)\\
\frac{d\Gamma_S^1}{ds} &= \left(-\frac{c^3}{\gamma_1\rho}+\frac{\gamma_1}{\rho c}(H-E_c)^2\right)\frac{d\varphi_{\alpha-\beta}}{d\xi}\frac{d\xi}{ds}\\
&\quad(\quad \text{using}\quad u\ \sin(\alpha-\beta)-v\ \cos(\alpha-\beta)+c=0)\\
\frac{d\Gamma_S^1}{ds} &= 0\\
\frac{d\Gamma_S^2}{ds} &= \frac{d\psi_1}{ds}+u\frac{d\psi_2}{ds}+v\frac{d\psi_3}{ds}+E_c\frac{d\psi_4}{ds}\\
\frac{d\Gamma_S^2}{ds} &= \left(\frac{c}{\rho}(1+\frac{\gamma_1}{2}M^2)+u(\frac{1}{\rho}(\sin(\alpha-\beta)-\gamma_1\frac{u}{c}))+v(\frac{1}{\rho}(-\cos(\alpha-\beta)-\gamma_1\frac{v}{c}))+E_c(\frac{\gamma_1}{\rho c})\right)\frac{d\varphi_{\alpha-\beta}}{d\xi}\frac{d\xi}{ds}\\
\frac{d\Gamma_S^2}{ds} &= \left(\frac{\gamma_1E_c}{\rho c}-\frac{\gamma_1u^2}{\rho c}-\frac{\gamma_1v^2}{\rho c}+\frac{\gamma_1E_c}{\rho c}\right)\frac{d\varphi_{\alpha-\beta}}{d\xi}\frac{d\xi}{ds}\\
&\quad(\quad \text{using}\quad u\ \sin(\alpha-\beta)-v\ \cos(\alpha-\beta)+c=0)\\
\frac{d\Gamma_S^2}{ds} &= 0
\end{aligned}
$$

Besides

$$
\begin{aligned}
\frac{d\Gamma_{C+}}{ds} &= (u+vt^+)\frac{d\psi_1}{ds}+(u^2+v^2)\frac{d\psi_2}{ds}+(u^2+v^2)t^+\frac{d\psi_3}{ds}+H(u+vt^+)\frac{d\psi_4}{ds}\\
\frac{d\Gamma_{C+}}{ds} &= ((u+vt^+)(\frac{c}{\rho}(1+\frac{\gamma_1}{2}M^2))+(u^2+v^2)(\frac{1}{\rho}(\sin(\alpha-\beta)-\gamma_1\frac{u}{c}))\\
&\quad+(u^2+v^2)t^+(\frac{1}{\rho}(-\cos(\alpha-\beta)-\gamma_1\frac{v}{c}))+H(u+vt^+)(\frac{\gamma_1}{\rho c}))\frac{d\varphi_{\alpha-\beta}}{d\xi}\frac{d\xi}{ds}
\end{aligned}
$$

It is easily checked that the first and fourth terms in the bracket are equal. After lengthy calculations using the null eigenvalues properties and then the formulas for the difference of cos and difference of sin, it appears that $d\Gamma_{C+}/ds = 0$. For the sake of brevity, the detail of the calculations is not shown here.

Biblography

References

[1] Jameson, A. Aerodynamic design via control theory. *Journal of Scientific Computing* **3**(3), 233–260 (1988).

[2] Anderson, W. and Venkatakrishnan, V. Adjoint design optimization on unstructured grid using a continuous adjoint formulation. In *AIAA Paper Series, Paper 1997-0643*. (1997).

[3] Anderson, W., , and Venkatakrishnan, V. Adjoint design optimization on unstructured grid using a continuous adjoint formulation. *Computers & Fluids* **28**, 443–480 (1999).

[4] Giles, M. and Pierce, N. Adjoint equations in CFD: Duality, boundary conditions and solution behaviour. In *AIAA Paper Series, Paper 97-1850*. (1997).

[5] Giles, M. and Pierce, N. Analytic adjoint solutions for the quasi-one-dimensional Euler equations. *Journal of Fluid Mechanics* **426**, 327–345 (2001).

[6] Baeza, A., Castro, C., Palacios, F., and Zuazua, E. 2d Euler shape design on non-regular flows using adjoint Rankine-Hugoniot relations. *AIAA Journal* **47**(3), 552–562 (2009).

[7] Coquel, F. and Marmignon, C. and Rai, P. and Renac, F. Adjoint approximation of nonlinear hyperbolic systems with non-conservative products. In XVII International Conference on Hyperbolic Problems: Theory, Numerics, Applications, Bressan, A., Lewicka, M., Wang, D., and Zheng, Y., editors, 385–392. AIMS, (2018).

[8] Lozano, C. Singular and discontinuous solutions of the adjoint Euler equations. *AIAA Journal* **56**(11), 4437–4451 (2018).

[9] Peter, J., Renac, F., and Labbé, C. Analysis of finite-volume discrete adjoint fields for two-dimensional compressible Euler flows. *Journal of Computational Physics* **449**, 110811 (2022).

[10] Lozano, C. Watch your adjoints! lack of mesh convergence in inviscid adjoint solutions. *AIAA Journal* **57**(9), 3991–4006 (2019).

[11] Peter, J. Contributions to discrete adjoint method in aerodynamics for shape optimization and goal-oriented mesh adaptation. University of Nantes. Mémoire pour Habilitation à Diriger des Recherches, (2020).

[12] Ferri, A. Application of the method of characteristics to supersonic rotational flow. Technical Report 841, NASA, (1946).

[13] Shapiro, A.H. *The Dynamics and Thermodynamics of Compressible Fluid Flow*. The Ronald Press Company, (1954).

[14] Bonnet, A. and Luneau, J. *Aérodynamique. Théories de la dynamique des fluides.* Cepadues, (1989).

[15] Délery, J. *Traité d'aérodynamique compressible. Volume 3*. Collection mécanique des fluides. Lavoisier – Hermés Science, (2008).

[16] Liepmann, H.W. and Roshko, A. *Elements of Gasdynamics*. Dover Publications, (1956).

[17] Anderson, J. *Modern Compressible Flow (third edition)*. McGraw-Hill series in Aernautical and Aerospace Engineering, (2003).

[18] Sears, W.R. (Under the editorial direction of). *General theory of high speed aerodynamics. Vol VI High speed aerodynamics and jet propulsion*. Princeton University Press, (1954).

[19] Venditti, D. and Darmofal, D. Grid adaptation for functional outputs: Application to two-dimensional inviscid flows. *Journal of Computational Physics* **176**, 40–69 (2002).

[20] Todarello, G., Vonck, F., Bourasseau, S., Peter, J., and Désidéri, J.-A. Finite-volume goal-oriented mesh-adaptation using functional derivative with respect to nodal coordinates. *Journal of Computational Physics* **313**, 799–819 (2016).

[21] Sartor, F. *Unsteadiness in transonic shock-wave/boundary layer interactions: experimental investigation and global stability analysis*. PhD thesis, Université Aix-Marseille, (2014).

[22] Sartor, F. and Mettot, C. and Sipp, D. Stability, Receptivity, and Sensitivity Analyses of Buffeting Transonic Flow over a Profile. *AIAA Journal* **53**(7), 1980–1993 (2010).

[23] Hirsch, Ch. *Numerical Computation of Internal and External Flows: The Fundamentals of Computational Fluid Dynamics (second edition)*. Butterworth – Heineman. Elsevier, (2007).

[24] Jameson, A., Schmidt, W., and Turkel, E. Numerical solutions of the Euler equations by finite volume methods using Runge-Kutta time-stepping schemes. In *AIAA Paper Series, Paper 1981-1259*. (1981).

[25] Peter, J. and Dwight, R. Numerical sensitivity analysis for aerodynamic optimization: a survey of approaches. *Computers and Fluids* **39**, 373–391 (2010).

[26] Peter, J., Renac, F., Dumont, A., and Méheut, M. Discrete adjoint method for shape optimization and mesh adaptation in the *elsA* code. status and challenges. In *Proceedings of 50th 3AF Symposium on Applied Aerodynamics, Toulouse*, (2015).

[27] Mohammadi, B. and Pironneau, O. *Applied Shape Optimization for Fluids*. Oxford Univ. Press, May (2001).

[28] Alauzet, F. and Pironneau, O. Continuous and discrete adjoints to the Euler equations for fluids. *Int. J. Numer. Meth. Fluids* **70**, 135–157 (2012).

[29] Lozano, C. A note on the dual consistency of the discrete adjoint quasi-one dimensional Euler equations with cell-centred and cell-vertex central discretization. *Computers and Fluids* **134-135**, 51–60 (2016).

[30] Vassberg, J. and Jameson, A. In pursuit of grid convergence for two-dimensional Euler solutions. *Journal of Aircraft* **47**(4), 1152–1166 (2010).